Functional divergence of the *bag of marbles* gene in the *Drosophila melanogaster* species group

Jaclyn E. Bubnell[1*], Cynthia K.S. Ulbing[1], Paula Fernandez Begne[1], and Charles F. Aquadro[1*]

[1] Department of Molecular Biology and Genetics, Cornell University, Ithaca, NY, USA

*Correspondence: Jaclyn Bubnell, jeb486@cornell.edu and Charles Aquadro, cfa1@cornell.edu

Authors performed the following: JEB - conceptualization, investigation, validation, formal analysis, and writing. CKSU and PFB - investigation, and validation, CFA - conceptualization, funding acquisition, supervision, and writing.

Abstract

In *Drosophila melanogaster,* a key germline stem cell (GSC) differentiation factor, *bag of marbles* (*bam*) shows rapid bursts of amino acid fixations between sibling species *D. melanogaster* and *D. simulans*, but not in the outgroup species *D. ananassae*. We previously hypothesized that a change in function and/or a genetic conflict with the intracellular bacteria *W. pipientis* could be driving the adaptive evolution of *bam*, however *bam* function has only been defined in *D. melanogaster*. Here, we test the null hypothesis that *bam'*s differentiation function is conserved in four additional *Drosophila* species in the *melanogaster* species group spanning approximately 15 million years of divergence. Surprisingly, we demonstrate that *bam* is not necessary for oogenesis or spermatogenesis in *D. teissieri* nor is *bam* necessary for spermatogenesis in *D. ananassae*. Remarkably *bam* function may change on a relatively short time scale. We further report tests of neutral sequence evolution at *bam* in additional species of *Drosophila* and find a positive correlation between evidence for positive selection at *bam* and its essential role in GSC regulation and fertility for both males and females. Further characterization of *bam* function in more divergent lineages will be necessary to distinguish between *bam's* critical gametogenesis role being newly derived in *D. melanogaster*, *D. simulans* and *D. yakuba* or it being basal to the genus and subsequently lost in numerous lineages.

Introduction

In most sexually reproducing animals, egg and sperm production begins with the differentiation of germline stem cells. These germline stem cells (GSCs) divide both to self-renew to maintain the germline and to produce daughter cells that differentiate to produce gametes (Kahney et al. 2019). The cellular processes of daughter cell differentiation and stem cell self-renewal are the most fundamental functions of stem cells and are therefore highly regulated and presumed to be conserved. In the germline the mis-regulation of either of these processes leads to sterility (Gleason et al. 2018). However, many of the genes that control GSC maintenance and GSC daughter differentiation in *D. melanogaster* are rapidly evolving due to positive selection for amino acid diversification (Civetta et al. 2006; Bauer DuMont et al. 2007; Choi and Aquadro 2015; Flores, DuMont, et al. 2015).

One such gene is *bag-of-marbles* (*bam*) which exhibits a rapid burst of amino acid substitutions between the sister species *D. melanogaster* and *D. simulans*, acts as the key switch for GSC daughter cell differentiation in *D. melanogaster* females, and is necessary for terminal differentiation of spermatogonia in males (McKearin and Spradling 1990; Civetta et al. 2006; Bauer DuMont et al. 2007; Insco et al. 2009). In females, *bam* is repressed in GSCs, and upon its expression promotes differentiation by binding to the protein product of *benign gonial cell neoplasm* (*bgcn)* as well as a series of other protein partners to repress the translation of self-renewal factors *nanos* and *eIF4a* (Li et al. 2009; Ting 2013). The GSC daughter cell differentiates into a cystoblast,

69 which then goes through four rounds of mitotic divisions while *bam* localizes to the
70 fusome, a cellular structure that interconnects the resulting dividing cells that make up
71 the cyst. In these cells, Bam functions with Bgcn to regulate mitotic synchrony (Chen
72 and McKearin 2003). Before meiosis begins, *bam* expression is repressed. In males,
73 *bam* is expressed in GSCs and its expression increases as differentiation progresses
74 (Insco et al. 2009). In early dividing spermatogonia, Bam protein must reach a threshold
75 to bind with partners Bgcn and *tumorous testis* (*tut*) to repress *mei-P26* and switch the
76 cellular program from proliferation to terminal differentiation to begin meiosis (Chen et
77 al. 2014). After this switch, *bam* expression is rapidly repressed. Loss of *bam* function in
78 either sex daughter cell differentiation and results in the over-proliferation of either
79 GSCs in females or spermatogonia in males causing tumors and sterility (McKearin and
80 Spradling 1990). The intriguing observation that *bam* is both rapidly evolving due to
81 positive selection and functions as a switch for GSC daughter differentiation has led us
82 to investigate what could be driving its adaptive evolution (Flores, Bubnell, et al. 2015).
83
84 One possibility is that the maternally inherited, endosymbiotic bacterium *Wolbachia*
85 *pipientis* is driving the evolution of *bam*. We previously identified a genetic interaction
86 between *bam* and *W. pipientis* (Werren et al. 2008) where infection with the *w*Mel strain
87 of *W. pipientis* partially rescued the fertility and cellular GSC daughter differentiation
88 defects of a *bam* partial loss-of-function mutant (hypomorph) in *D. melanogaster*
89 females (Flores, Bubnell, et al. 2015; Bubnell et al. 2021). That *W. pipientis* rescues a
90 *bam* hypomorph in females, and that functional consequences of *bam* divergence
91 between *D. melanogaster* and *D. simulans* is female specific, are consistent with the

92 possibility that interactions between the *Drosophila* germline and *W. pipientis* could
93 drive positive selection at *bam.*
94
95 Another possible explanation for the observed signal of positive selection at *bam* is a
96 change of function. As *bam* regulates gametogenesis, it is possible that life history or
97 environmental factors drive positive selection at *bam*. It is even possible that the genetic
98 interaction between *Wolbachia* and *bam* has led to such changes in *bam*'s function in
99 different lineages. While functional divergence of *bam* seems less likely due to its
100 essential role in GSC maintenance and differentiation in *D. melanogaster, bam*
101 sequence is highly divergent among species, making it even difficult to confidently align
102 between *D. melanogaster* and *D. ananassae,* both members of the *melanogaster*
103 species group (subgenus Sophophora), let alone the many more divergent Drosophila
104 species (Bauer DuMont et al. 2007). Additionally, *bam* appears to be a novel gene in
105 the genus *Drosophila* as no orthologues are reported in any non-Drosophila genomes
106 using orthoDB v10 (Kriventseva et al. 2019) and Ensembl Metazoa (Howe et al. 2020)
107 (both accessed 11/4/2021).
108
109 Here, we ask if *bam* is necessary for gametogenesis in diverse species within the
110 *Drosophila* genus. We generate *bam* loss-of-function alleles in five *Drosophila* species
111 in the *melanogaster* group. Surprisingly, we find that *bam* is not necessary for
112 gametogenesis in one or both sexes in two species within the *melanogaster* group. We
113 also analyze additional population samples of species mainly within the *melanogaster*
114 species group and a few more distant lineages for nucleotide sequence variation at

115 *bam.* Within the *melanogaster* species subgroup, we find evidence of lineage-specific
116 signals of adaptation for four species, but not for *D. teissieri*. Outside of the
117 *melanogaster* species subgroup, we find no departures from selective neutrality in the
118 four species we analyzed. Together with our *bam* loss-of-function results, these
119 observations raise the possibility that the critical role of *bam* in GSC differentiation is
120 newly derived in the *melanogaster* species group and the signatures of positive
121 selection we observe in some of those species is associated with species-specific
122 refinements of *bam*'s GSC differentiation function.
123

124 ## Results

125

126 **Generating *bam* null alleles for non-*melanogaster* species**

127 To ask if *bam's* GSC function is conserved in species outside of *D. melanogaster*, we
128 designed and generated a series of *bam* null alleles in five species in the *melanogaster*
129 species group to assay for GSC daughter differentiation (Fig 1A). To do this, we used
130 CRISPR/Cas9 to introduce a 3xP3-YFP or a 3xP3-DsRed gene cassette into the first
131 exon of *bam*, thereby disrupting the *bam* coding sequence and introducing a premature
132 termination codon (Fig 1B). This also generates an allele that is trackable by eye color,
133 which is necessary for the non-*melanogaster* species of which we do not have balancer
134 chromosomes to maintain alleles that cause sterility. Being able to track the null allele is
135 a concern in this design if *bam* is necessary for GSC daughter differentiation in the
136 species tested, because a loss of function allele will cause sterility (as it does in *D.*
137 *melanogaster* males and females). To generate the homozygous *bam* null genotype, we

138 cross the 3xP3-YFP line to the 3xP3-DsRed line and select flies with both DsRed and
139 YFP positive eyes. This scheme also allows us to use the same cross to assay the
140 heterozygous and wildtype *bam* siblings (Table 1).
141
142 We used *D. melanogaster* as a control to ensure our method would generate a loss of
143 function *bam* phenotype, as the *bam* null phenotype has been well characterized in this
144 species (Table 1). We also generated *bam* nulls in four other species within the
145 *melanogaster* species group *D. simulans*, *D. yakuba*, *D. teissieri,* and *D. ananassae*
146 (Fig 1A).
147
148 ***bam* is necessary for female and male fertility in *D. melanogaster*, *D. simulans*,**
149 **and *D. yakuba*, but only in *D. ananassae* females, and in neither *D. teissieri* males**
150 **nor females.**
151 In *D. melanogaster*, both male and female *bam* nulls are sterile as early germline cells
152 fail to differentiate and proceed through gametogenesis. In classic null alleles of *D.*
153 *melanogaster bam* ($bam^{\Delta 59}$ and $bam^{\Delta 86}$), one copy of functional *bam* is sufficient to
154 rescue the *bam* null sterility phenotype. We first asked if our novel *bam* null alleles
155 behaved this way in *D. melanogaster*. We found that in both males and females,
156 heterozygotes of each 3xP3-DsRed or 3xP3-YFP disruption line showed similar fertility
157 to wildtype *bam* and that flies carrying both the 3xP3-DsRed and the 3xP3-YFP
158 disruptions (which we will term the *bam* null genotype) was completely sterile (Fig 2, Fig
159 S1, File S2). We observed this same pattern for *D. simulans* and *D. yakuba* (Fig 2, Fig
160 S1, File S2). However, when we assessed fertility of the *D. teissieri bam* null, we found

161 that there was no difference in fertility between any of the genotypes tested for females
162 or males (Fig 2, Fig S1, File S2). The *bam* null genotype did not result in sterility, or
163 even reduced fertility. In *D. ananassae*, *bam* null females were sterile, and one copy of
164 the null allele of each 3xP3-DsRed or 3xP3-YFP disruption did not significantly reduce
165 fertility, but in *D. ananassae* males, *bam* nulls were fertile, with no significant mean
166 difference in progeny across the tested genotypes (Fig 2, Fig S1, File S2). Therefore,
167 *bam* is not necessary for fertility in all species in the *melanogaster* species group, or
168 even all species within the *melanogaster* species subgroup.
169
170 **Consistent with the fertility results, *bam* is also necessary for germ cell**
171 **differentiation in *D. simulans* and *D. yakuba* females and males, but not in *D.***
172 ***teissieri* males or females, and only *D. ananassae* females.**
173 In *D. melanogaster* females, *bam* null ovaries feature over-proliferating germline stem
174 cells that fail to differentiate into cystoblasts (McKearin and Spradling 1990; Ting 2013).
175 This results in the germarium and developing downstream cysts accumulating small,
176 GSC-like cells resembling tumors (Fig 3A). In *D. melanogaster bam* null males,
177 spermatogonia differentiation is blocked which results in testes with over-proliferating
178 spermatogonia that fail to develop into terminally differentiated spermatocytes (Fig 3A)
179 (Insco et al. 2009; Insco et al. 2012).
180
181 We imaged ovaries from 2-5 day old *D. melanogaster* females from each *bam*
182 genotype. We assayed for the characteristic *bam* null tumor phenotype using antibodies
183 to Vasa to visualize the morphology of the germline and Hts-1B1 to visualize the

184 fusome, which fails to fully form in *bam* mutants (Lavoie et al. 1999; Hinnant et al.
185 2020). We found that the *bam* null genotype resulted in the characteristic *bag of*
186 *marbles* phenotype consistent with classic *bam* null alleles, with tumorous ovaries filled
187 with undifferentiated GSC-like cells (Fig 3B). One copy of wildtype *bam* was sufficient to
188 rescue the *bam* null phenotype, as has been previously observed for other *bam* null
189 alleles (Fig 3B) (Lavoie et al. 1999; Flores, Bubnell, et al. 2015). Therefore, our 3xP3-
190 DsRed and 3xP3-YFP disruptions successfully recapitulate the *bam* null phenotype in
191 females. We imaged testes from 3-5 day old *D. melanogaster* males and also
192 immunostained with antibodies to Vasa to label the germline and Hts-1B1 to label the
193 fusome. We found that the *bam* null genotype resulted in tumorous testes filled with
194 small over-proliferating cells that fail to differentiate into spermatocytes (Fig 3B). We
195 found that one copy of wildtype *bam* was sufficient to rescue the *bam* null tumor
196 phenotype, as has been previously reported for classic *bam* null alleles (Gönczy et al.
197 1997; Shivdasani and Ingham 2003)(Fig 3B). Therefore, our *bam* null alleles also
198 recapitulate the previously described *bam* null phenotype in *D. melanogaster* males.
199
200 We repeated the same analysis for the other species in the study. We found for *D.*
201 *simulans* and *D. yakuba* both female and male homozygous *bam* null genotypes
202 exhibited the characteristic ovarian and testes tumors as described in *D. melanogaster*
203 (Fig 3B). In these two species for both males and females, one copy of *bam* was also
204 sufficient to rescue the *bam* null phenotype as observed in *D. melanogaster* (Fig 3B).
205 However, in the *D. teissieri bam* null genotype, we observed no evidence of GSC over-
206 proliferation in females or spermatogonia over-proliferation in males. We observe the

207 same phenotype for the heterozygous alleles in both males and females, as well as
208 wildtype (Fig 3B). This indicates that *bam* is not necessary for GSC daughter
209 differentiation in *D. teissieri* females nor is *bam* necessary for spermatogonia
210 differentiation in males. In *D. ananassae bam* null females, we observed the
211 characteristic *bam* null phenotype observed in *D. melanogaster* with over-proliferating
212 GSC-like cells in the germarium and cysts and undeveloped fusomes (Fig 3B). One
213 copy of *bam* was sufficient to rescue the *bam* null tumorous phenotype (Fig 3B).
214 Therefore the *D. ananassae* female *bam* null phenotype is consistent with that of *D.*
215 *melanogaster*, *D. simulans*, and *D. yakuba*. In contrast, in *D. ananassae* males of the
216 *bam* null genotype we did not observe over-proliferating spermatogonia (Fig 3B). The
217 homozygous *bam* null genotype resulted in the same phenotype as the heterozygous
218 bam null genotypes and wildtype indicating that *bam* is not necessary for the switch
219 from proliferating spermatogonia to differentiated spermatocytes in *D. ananassae*
220 males. Therefore, these cytological data are fully consistent with our fertility assay
221 observations.
222
223 **Confirming the loss-of-function status of *bam* in the *bam* null disruption design**
224 The only available Bam antibody is weak in *D. melanogaster* and *D. simulans* thus we
225 cannot directly demonstrate the absence of Bam protein in all the species tested.
226 Although we used the same design to generate the *bam* null alleles across this study
227 and therefore expect the 3xP3-DsRed and 3xP3-YFP disruptions to have the same
228 effect on *bam* in all five species, we further confirmed the loss-of-function status of the
229 *bam* disruption alleles in *D. ananassae* and *D. teissieri* given their functional divergence.

230

231 First, we asked if *bam* had undergone duplication events in *D. ananassae* and *D.*
232 *teissieri* using publicly available sequence data and found no evidence of *bam*
233 duplication in either species (details described in S1 File, S8 Table). Next, since the
234 3xP3-DsRed and 3xP3-YFP insertions introduce a premature termination codon, we
235 expect the mRNA of the disrupted *bam* allele to be degraded through nonsense
236 mediated mRNA decay (NMD), but if the premature termination codon induced exon
237 skipping, the disrupted *bam* exon could be alternatively spliced out resulting in
238 expression of a truncated *bam* allele, which may be sufficient for function (Brogna and
239 Wen 2009; Mou et al. 2017; Chen et al. 2018; Sui et al. 2018). We used RT-qPCR to
240 ask if patterns of expression in the *bam* null alleles in *D. ananassae* males and *D.*
241 *teissieri* females and males were consistent with expectations for NMD. We found that
242 for *D. ananassae* and *D. teissieri*, the expression of the *bam* null disruption alleles were
243 reduced relative to the *bam* wildtype allele to levels consistent with NMD (~1-50%,
244 details in S1 File, Fig S2) (Pereverzev et al. 2015). Therefore, the mRNA of the *bam*
245 disruption alleles are likely targeted for degradation. Additionally, since both *bam* null *D.*
246 *teissieri* males and females show wildtype phenotypes, we asked if the exon disrupted
247 by 3xP3-YFP or 3xP3-DsRed in the *bam* null genotypes was expressed in proportion to
248 the non-disrupted exons relative to the wildtype genotype to look for evidence of exon
249 skipping. We found that the ratio of exon 1 to exon 2 expression was not significantly
250 different between *D. teissieri* nulls and *D. teissieri* wildtype genotypes for males and
251 females (details in S1 File, FigS4).

252

253 Although *bam* null *D. ananassae* males and *D. teissieri* males and females exhibited
254 wildtype phenotypes, together the genomic and RT-qPCR analyses indicate that the
255 *bam* null alleles are loss-of-function alleles. This evidence therefore supports our
256 conclusion that *bam* is not required for spermatogenesis in *D. ananassae* and *D.*
257 *teissieri* nor oogenesis in *D. teissieri.*
258
259 ***D. ananassae bam* null males show evidence of germline defects**
260 As we found that *bam* was necessary for oogenesis in *D. ananassae* but not for
261 spermatogenesis, we assayed for more subtle evidence of germline defects in *D.*
262 *ananassae* males by immunostaining testes with an antibody to Fas3 which is
263 expressed in epithelial cells in the hub, the testes microenvironment that houses the
264 somatic and germline stem cell populations. In *D. melanogaster bam* null males, Fas3 is
265 mis-expressed outside of the hub, as the spermatogonia over proliferate (Fig 4A&B). In
266 *D. ananassae bam* null males, we also observed misexpression of Fas3 outside of the
267 hub, although not nearly as severe as in *D. melanogaster bam* null males (Fig 4C&D).
268 This indicates that while *bam* is not necessary for differentiation in *D. ananassae* males,
269 it may be playing a role in maintenance of the stem cell population.
270
271 ***bam* shows lineage-specific bursts of positive selection in the *yakuba* complex,**
272 **and no evidence of positive selection outside of the *melanogaster* species**
273 **subgroup**
274 Previously, our group found that *bam* is evolving under strong positive selection
275 detected by the McDonald-Kreitman test in *D. melanogaster* and *D. simulans*, but not in

276 *D. ananassae* (Bauer DuMont et al. 2007; Choi and Aquadro 2014). As these three
277 species span about 15 million years of divergence, we wanted to know if there was
278 evidence of adaptation in lineages more closely related to *D. melanogaster* and *D.*
279 *simulans*, or if this signal was unique to the individual *D. melanogaster* and *D. simulans*
280 lineages. We expanded the species sampled to include three closely related species
281 from the *yakuba* complex: *D. yakuba, D. santomea,* and *D. teissieri*. We also took
282 advantage of published population genomic data from large samples of inbred lines to
283 expand our assessment of *bam* variation in an additional population sample each for *D.*
284 *melanogaster* and *D. simulans*.
285
286 In addition to further sampling more closely related species to *D. melanogaster* and *D.*
287 *simulans,* we also wanted to ask if there was any evidence of adaptive evolution at *bam*
288 in lineages outside of the *melanogaster* group. We resequenced *bam* from population
289 samples of three more distantly related *Drosophila* species: *D. pseudoobscura*, *D.*
290 *affinis*, and *D. mojavensis* which span approximately 40 million years of divergence
291 (Clark et al. 2007).
292
293 To ask if any population samples showed departures from selective neutrality consistent
294 with positive selection at *bam* similar to what we previously observed for *D.*
295 *melanogaster* and *D. simulans*, we used a lineage-specific McDonald-Kreitman test
296 (MKT) (Siddiq et al. 2017). The null hypothesis of the MKT is that the ratio of
297 nonsynonymous to synonymous polymorphism within a species is equal to the ratio of
298 nonsynonymous to synonymous fixed differences between species (or in our case, a

299 predicted common ancestral sequence). Previously, we have detected signatures of
300 positive selection at *bam* as an excess of nonsynonymous fixations in the *D.*
301 *melanogaster* and *D. simulans* lineages (Bauer DuMont et al. 2007). As *bam* appears to
302 be experiencing episodic signals of adaptive evolution restricted to individual lineages,
303 we measured lineage-specific divergence. We used codeml to generate reconstructed
304 ancestral sequences at the node of interest by maximum likelihood (Yang 1997; Yang
305 2007). We then used this sequence to calculate nonsynonymous and synonymous
306 divergences for each population sample.
307
308 For *D. melanogaster*, we utilized the Zambia population sample from the *Drosophila*
309 genome Nexus to measure *bam* variation (Lack et al. 2015). The Zambia sample
310 contains the largest sample size of intact *bam* sequence (few missing calls), and
311 represents variation found in the ancestral range of *D. melanogaster*. We used the
312 predicted common ancestor of *D. melanogaster* and *D. simulans* and found similar
313 patterns of polymorphism and divergence to the smaller samples of *D. melanogaster*
314 from the USA and Zimbabwe previously reported by Bauer DuMont et al. (Bauer
315 DuMont et al. 2007) (Fig 5). The *D. melanogaster* lineage shows a strong signal of
316 adaptive evolution (alpha = 0.912, P<0.000) (Fig 5).
317
318 For *D. simulans bam*, we utilized the CA, USA population sample from Signor et al
319 (Signor et al. 2018). The previous *D. simulans bam* sample our lab reported was also
320 from the USA, but from North Carolina (Aquadro et al. 1988; Bauer DuMont et al. 2007).
321 We used the same common ancestral sequence as we did for the *D. melanogaster*

322 analysis to calculate divergence. However, we did not observe the same patterns of
323 divergence and polymorphism in this sample as we previously observed in the NC
324 sample (Fig 5). In the CA *bam* sample, we cannot reject neutrality (alpha = 0.539,
325 P=0.084), in contrast to our previous finding in the NC sample (alpha=0.631, P=0.049).
326 It is notable that although the ratios were not significantly different, the trend in this
327 lineage also shows a high alpha value and higher nonsynonymous divergences. The
328 difference between the two samples seems to be driven by higher nonsynonymous
329 polymorphism in the CA sample compared to the NC sample.
330
331 We used the predicted common ancestor of the *yakuba* complex (*D. yakuba*, *D.*
332 *santomea*, *D. teissieri*) to estimate divergence for *bam* in each of the population
333 samples. For *D. yakuba* and *D. santomea* we also observed significant signals of
334 positive selection for *bam* (*D. yakuba*: alpha=0.723, P=0.006; and *D. santomea*:
335 alpha=0.726, P=0.024) (Fig 5). In contrast, we could not reject neutrality for *D. teissieri*
336 *bam* and the estimate of alpha is very low (alpha=-0.011, P=0.983) (Fig 5).
337
338 In lineages outside of the *melanogaster* species subgroup, we did not reject neutrality at
339 *bam* for any of the species we sampled. For *D. ananassae*, we reassessed divergence
340 with the predicted common ancestor of *D. atripex* and *D. ananassae* to further polarize
341 the patterns of divergence in the *D. ananassae* lineage as Choi et al. (Choi and
342 Aquadro 2014) reported divergence between *D. ananassae* and *D. atripex*. Our findings
343 are consistent with the previous study (alpha = 0.816, P= 0.089) (Choi and Aquadro
344 2014). The alpha value is high here although not significant, which suggests it may be

345 informative to sample *bam* from additional *D. ananassae* populations with larger sample
346 sizes (n=14 here). We calculated divergence for *bam* from population samples of *D.*
347 *pseudoobscura* and *D. affinis* from their predicted common ancestor and observed
348 similar patterns of polymorphism and divergence (*D. pseudoobscura*: alpha=0.250,
349 P=1), (*D. affinis*: alpha=0.487, P=0.360), neither of which were close to rejecting neutral
350 expectations (Fig 5). We used the predicted common ancestor of *D. mojavensis* and *D.*
351 *arizonae bam* to calculate divergence in the *D. mojavensis* lineage and again did not
352 observe a trend towards an excess of nonsynonymous divergence (alpha=0.250, P=1)
353 (Fig 5). Therefore, the only species for which we have observed evidence of positive
354 selection remain the in the *melanogaster* species subgroup.
355

356 ## Discussion

357

358 **Bam's role in germline stem cell maintenance and differentiation shows**
359 **remarkable variation in the *Drosophila melanogaster* species group.**
360 Our comparative assessment of *bam* requirement in gametogenesis across diverse
361 *Drosophila* species indicates that the functional evolution of *bam* is unexpectedly
362 complex. We discovered that *D. teissieri* and *D. ananassae* do not require *bam* for
363 gametogenesis in one or both sexes. These results raise the question as to whether
364 *bam*'s critical role in GSC differentiation originally characterized in *D. melanogaster* is in
365 fact a phylogenetically recent gain of function, or whether *bam*'s critical role is basal to
366 the genus (as a *bam* orthologue is found throughout the genus) and that *bam*'s role has
367 been recently (and possibly repeatedly) lost in specific lineages. For example, assuming

368 *bam*'s role in GSC differentiation is basal, then the most parsimonious explanation of
369 our functional data is that *bam* was required for oogenesis and spermatogenesis in the
370 common ancestor of the species tested (Fig 1A), then *bam* function was lost in *D.*
371 *ananassae* males, and then lost again independently in *D. teissieri* males and females.
372 These alternative scenarios can be distinguished by the follow-up examination of *bam*
373 function in more divergent *Drosophila* species.
374
375 **There is evidence of positive selection for protein diversification at Bam only in**
376 **four of the *melanogaster* group species.**
377 We analyzed additional population samples of species mainly within the *melanogaster*
378 species group and a few more distant lineages for nucleotide sequence variation at
379 *bam.* We find new evidence of lineage-specific signals positive selection for accelerated
380 protein sequence evolution at *bam* in four of the *melanogaster* species subgroup
381 species (*D. melanogaster, D. simulans* (NC sample)*, D. yakuba,* and *D. santomea*), but
382 we do not detect signals in *D. teissieri* or outside of the *melanogaster* species subgroup
383 including *D. ananassae*, *D. pseudoobscura*, *D. affinis* and *D. mojavensis*.
384
385 The failure to reject selective neutrality for *bam* in the *D. simulans* population sample
386 from CA appears to be due to a recent non-equilibrium population history for the
387 California sample. There is a genome-wide excess of intermediate frequency
388 polymorphisms in the CA population sample that is consistent with a combination of
389 population contraction and possibly soft sweeps on standing genetic variation within the
390 past 100 years in this CA *D. simulans* population (Signor et al. 2018). The introduction

391 of the *w*Ri strain of *W. pipientis* into southern CA around the 1980s led to the spread of
392 this strain through CA with initially strong Cytoplasmic Incompatibility (Hoffmann et al.
393 1986) that would have also resulted in a severe bottleneck particularly in the female
394 effective population size (e.g. (Cariou et al. 2017)). A population bottleneck can bring
395 slightly deleterious polymorphisms to higher frequency. While the frequency of these
396 deleterious polymorphisms will then slowly decline, during this time their frequency in
397 the population is thus an overestimation of their probability of their fixation and thus
398 weaken power of the MKT and underestimate alpha (e.g. (Messer and Petrov 2013)). It
399 is important to note as well that the MKT has limited power statistically when applied to
400 single genes (Akashi 1999; Zhai et al. 2009) and thus a failure to reject selective
401 neutrality does not prove that positive selection is or has not acted on this gene.
402
403 **Are stem cell genes hotspots for adaptive evolution?**
404 The results of past studies of GSC evolution (Bauer DuMont et al. 2007; Choi and
405 Aquadro 2014; Choi and Aquadro 2015; Flores, DuMont, et al. 2015) and our population
406 genetic and functional results in this study lead to the question of why GSC
407 developmental functions are frequent targets of adaptation. Selfish transposable
408 elements are regulated by piRNAs to protect the germline genome (Aravin et al. 2007;
409 Simkin et al. 2013). There is natural variation in the gene *Bruno* that provides tolerance
410 to deleterious P-element expression in the genome (Kelleher et al. 2018). In a scRNA-
411 seq study of male *D. melanogaster* testes, Witt et al. (Witt et al. 2019) report many fixed
412 de novo genes expressed in GSCs and early spermatogonia (where *bam* is expressed)
413 at similar levels to testis specific genes. In contrast, segregating de novo genes show

414 lower expression in GSCs and early spermatogonia implying that cell type expression
415 may impact the likelihood for a de novo gene to become fixed. As de novo gene
416 evolution is increasingly recognized as a critical mode of adaptation, especially in
417 reproduction, GSCs/early spermatogonia may be generating necessary variation for
418 adaptation (Witt et al. 2019). A recent finding that the insect gene *oskar,* which is
419 critical for germ cell formation and oogenesis, arose *de novo* through a horizontal gene
420 transfer event from a prokaryote, resulting in a fusion between prokaryotic and
421 eukaryotic sequence illustrates yet another mechanism by which novel genes can take
422 on key developmental roles in reproduction (Jenny et al. 2006; Blondel et al. 2020).
423
424 The *bam* sequence itself has many properties of novel genes: it does not contain any
425 known DNA or RNA binding motifs, it binds with multiple protein partners, contains
426 structurally disordered regions, and is expressed in a tight spatiotemporal manner
427 (Chen et al. 2010; Jiang and Assis 2017; Wilson et al. 2017; Klasberg et al. 2018;
428 Vakirlis and McLysaght 2019). Novel genes that become fixed often gain critical roles in
429 conserved gene networks. Their new role may lead to selection to fine tune their critical
430 role thereby providing additional functional flexibility for these conserved processes
431 (Chen et al. 2010). Such a process could represent what has been called
432 developmental systems drift, a model to explain how developmental systems remain
433 phenotypically conserved while the genetic pathways that determine them diverge (True
434 and Haag 2001).
435

436 It is possible that *bam* was a novel gene to the common ancestor of *Drosophila* (and
437 possibly some other dipterans) and has functionally diversified across the *Drosophila*
438 genus, only gaining its role in germline stem cell differentiation in the lineage leading to
439 the *melanogaster* species group. Additionally, it is possible that *bam* quickly evolved a
440 role in GSC daughter differentiation in *Drosophila,* but that function has been shaped by
441 germline conflicts in specific lineages. Conflict with germline agents (such as *W.*
442 *pipientis)* may even drive the fixation of novel genes in new roles that successfully
443 evade their control.
444
445 It certainly seems plausible that genetic conflict is one way for new genes to evolve
446 required functions in conserved processes such as GSC daughter differentiation. The *D.*
447 *melanogaster* testes and the accessory gland show enriched expression of novel
448 genes, many of which show signals of adaptive evolution, and some of which are
449 predicted to be driven by sexual conflict (Levine et al. 2006; Zhou et al. 2008; Findlay et
450 al. 2009; Kaessmann 2010; Gubala et al. 2017; Witt et al. 2019). While the
451 developmental processes of gametogenesis and reproduction must be conserved, our
452 results demonstrate that the individual genes that function in that process may be vary
453 among even closely related species.
454

455 ## Materials and Methods

456

457 **Fly stocks and rearing:**

458 We raised fly stocks on standard cornmeal molasses food at room temperature. We
459 used yeast glucose food for fertility assays. The *D. melanogaster* w^{1118} isogenic line and
460 w^{1118} balancer lines were gifts from Luis Teixeira, and the *D. simulans* w^{501} line (stock
461 14021-0251.011), the *D. yakuba* white eyed line (14021-226.03) and the *D. ananassae*
462 reference genome (14024-0371.14) lines are from the Drosophila species stock center
463 (http://blogs.cornell.edu/drosophila/). The *W. pipientis*-free *D. ananassae* line Nou83
464 was a gift from Artyom Kopp. The *D. teissieri* line (*teissieri* syn) was a gift from Daniel
465 Matute (Turissini et al. 2015).
466
467 We tested all lines for *W. pipientis* infection status by qPCR (NEB Luna Universal qPCR
468 kit) using primer sets for *wsp* and *arm* (S1 Table). Lines that tested positive (*D. teissieri*,
469 *D. ananassae*, *D. simulans*) were treated with tetracycline (200 µg/mL) for three
470 generations to remove *W. pipientis* (Glover et al. 1990). We allowed these lines to
471 recover for at least three generations before using them in any analyses. We were
472 unable to fully clear the *D. ananassae* reference line of *W. pipientis* with tetracycline, so
473 to obtain a *W. pipientis* free stock, we crossed males of our *bam* null lines to females
474 from the Nou83 line, which we confirmed to be *W. pipientis*-free by qPCR.
475
476 **Cloning for bam null constructs**:
477 We obtained the nucleotide sequence information for designing constructs in *D.*
478 *melanogaster, D. simulans*, *D. yakuba*, and *D. ananassae* from FlyBase (Thurmond et
479 al. 2019). We obtained sequence information for the *D. teissieri* sequences from Daniel
480 Matute. We used Geneious for all cloning design.

481

482 We used the NEB Q5 High Fidelity 2X master mix to generate all PCR products. We gel
483 extracted and purified PCR products using the NEB Monarch DNA gel extraction kit or
484 Qiagen MinElute gel extraction kit. IDT primers were used for PCR, sequencing, and
485 cloning. We generated the donor plasmids for the 3xP3-DsRed and 3xP3-YFP bam
486 disruption lines using the NEB HiFi Assembly Cloning kit into the pHD-attP-DsRed
487 vector from flyCRISPR (Gratz et al. 2014) as follows: we amplified 1.5 kb homology
488 arms from genomic DNA of the appropriate species stock flanking the insertion site for
489 3xP3-DsRed or 3xP3-YFP. 3xP3-DsRed was amplified from the pHD-attP-DsRed
490 plasmid and 3xP3-YFP was amplified from the *D. simulans* nos-Cas9 line, a gift from
491 David Stern. We then gel extracted the two homology arms and the appropriate 3xP3
492 marker, purified them, and assembled them into the pHD vector backbone using the
493 manufacturer's protocol (S3 Table).

494

495 We used the U6:3 plasmid from CRISPRflydesign (Port et al. 2014) to express gRNAs
496 for generating the *D. yakuba* lines. The gRNA target sequence was generated by
497 annealing primers with the gRNA sequence and BbsI site overhangs, and ligating into
498 the BbsI ligated U6:3 vector (T4 ligase NEB, BbsI NEB) (S3 Table). We used NEBalpha
499 competent cells for transformations.

500

501 We prepped and purified all plasmids for embryo injections with the Qiagen plasmid
502 plus midi-prep kit. We additionally purified plasmids for injections with phenol-chloroform

503 extraction to remove residual RNases. We confirmed plasmid sequences with Sanger
504 sequencing (Cornell BRC Genomics Facility).
505
506 **CRISPR/Cas9:**
507 gRNA selection:
508 We chose gRNAs using the flyCRISPR target finder (Gratz et al. 2014) for *D.*
509 *melanogaster*, *D. simulans*, *D. yakuba*, and *D. ananassae*. For *D. teissieri*, we used one
510 completely conserved gRNA from *D. yakuba.* We also chose an additional gRNA from
511 *D. yakuba* that had two divergent sites between *D. yakuba* and *D. teissieri,* thus we
512 modified them to the *D. teissieri* sites. We selected gRNAs that had no predicted off-
513 targets in the reference genome (S4 Table & S5 Table). For *D. yakuba*, we used the
514 U6:3 gRNA plasmid from CRISPRfly design as described above. For the remaining
515 species (*D. melanogaster*, *D. simulans*, *D. teissieri*, and *D. ananassae*), we used
516 synthetic gRNAs (sgRNAs) from Synthego. We used 1-3 gRNAs per injection to
517 increase the chances of a successful CRISPR event. We used multiple gRNAs if there
518 were suitable options for that site to increase efficiency (multiple gRNAs within 50 bps
519 with 0 predicted off-targets).
520
521 Injections:
522 All CRISPR/Cas9 injections were carried out by Genetivision. Lines were injected with
523 the plasmid donor, gRNAs (synthetic or plasmid), Cas9 protein (Synthego), and an
524 siRNA for Lig4 (IDT DNA). The same siRNA was used for *D. melanogaster*, *D.*
525 *simulans*, *D. yakuba*, and *D. teissieri* (pers communication with Daniel Barbash and

526 David Stern S6 Table). We created a *D. ananassae* specific siRNA due to sequence
527 divergence (S6 Table).
528
529 For the *bam* disruption lines, we screened for eye color in F1s in house using a
530 Nightsea fluorescence system with YFP (cyan) and DsRed (green) filters. We
531 backcrossed all CRISPR/Cas9 mutants to the stock line we used for injections for three
532 generations. All mutants are maintained as heterozygous stocks. We confirmed all
533 CRISPR insertions by Sanger sequencing (Cornell BRC Genomics Core Facility).
534
535 <u>Genotypes for generating bam disruption homozygotes</u>:
536 We generated two *bam* disruption lines in each species in order to create the genotypes
537 for the comparative *bam* null analyses. We generated one by disrupting *bam* with 3xP3-
538 DsRed and the other with 3xP3-YFP. We selected DsRed or YFP positive flies and
539 crossed them to generate homozygous *bam* disruption flies ($bam^{3xp3\text{-}DsRed}/bam^{3xP3\text{-}YFP}$).
540 This cross also results in DsRed or YFP positive heterozygous *bam* null progeny as well
541 as *bam* wildtype progeny without any fluorescent eye marker.
542
543 We targeted the 1st exon of *bam* in all species in order to disrupt the *bam* coding
544 sequence and introduce an early stop codon. While we were successful in generating
545 1st exon disruptions in each species, in *D. simulans* we were only able to obtain a 3xP3-
546 YFP 1st exon disruption line. However, we did find that a *D. simulans* line with a 3xP3-
547 DsRed insertion in its 2nd intron resulted in homozygous sterile females and males with
548 tumorous ovaries and testes, while heterozygous females and males were fertile with

549 wildtype ovary and testes phenotypes. As this edit was specific to the *bam* locus, we
550 presumed it was an mRNA null allele and we used this line for our analyses. Thus, if the
551 phenotype of the 3xP3-DsRed 2nd intron allele over the 3xP3-YFP 1st exon allele is the
552 same as the homozygous 3xP3-DsRed 2nd intron allele, this is consistent with
553 classification as a genetic null.
554
555 **Fertility assays:**
556 Female fertility:
557 All female fertility assays were performed following the approach of Flores et al. (Flores,
558 Bubnell, et al. 2015). Specifically, we collected virgin females and aged them 2-3 days
559 (*D. melanogaster*, *D. simulans*, *D. yakuba,* and *D. teissieri*) or 5-7 days (*D. ananassae*).
560 We collected all genotypes from each bottle to control for bottle effects. We collected
561 virgin males of the wildtype genotype for each species and aged them for the same
562 timeframe as the females of that species. We evenly distributed males collected from
563 different bottles across the female genotypes to control for any bottle effects. We
564 crossed single females collected within 48 hours of each other to two virgin males. We
565 allowed the trio to mate for 9 days, and then flipped them to new vials. Except for *D.*
566 *ananassae* and *D. yakuba*, as fertility was very low, we cleared the trio after day 9 and
567 did not continue further. For all other species crosses, after an additional 9 days, we
568 cleared the trio. Then, we counted the progeny for each trio every two to three days to
569 get the total adult progeny per female.
570
571 Male fertility:

572 All male fertility assays were performed as described for the female fertility assays
573 except that one tester male was crossed to two virgin females.
574
575 Food and conditions for fertility assays:
576 For *D. melanogaster*, *D. simulans*, *D. ananassae*, and *D. teissieri*, we performed all
577 fertility assays on yeast-glucose food. For *D. yakuba*, we performed fertility assays on
578 cornmeal-molasses food, as this line did not thrive on the yeast-glucose food. We kept
579 all crosses and fertility experiments in an incubator at 25°C with a 12-hour light-dark
580 cycle.
581
582 **Statistics**:
583 For the fertility assays we used estimation statistics to assess the mean difference
584 (effect size) of adult progeny between the wildtype *bam* genotype and each individual
585 additional *bam* genotype. For generating the estimation statistics and plots (Ho et al.
586 2019), we used the dabest package in Python (v. 0.3.1) with 5,000 bootstrap resamples.
587 Estimation statistics provide a non-parametric alternative to other statistical tests of the
588 difference of the mean (for example, ANOVA), and allow us to understand the
589 magnitude of the effect of *bam* genotype on the fertility phenotype. In text, we report
590 significance as a mean difference (effect size) outside the 95% bootstrap confidence
591 interval. While one benefit of these statistics is that they are less biased than reporting
592 traditional P-values, we also report P-values for approximate permutation tests with
593 5,000 permutations.
594

595 **Immunostaining:**

596 We used the following primary antibodies, anti-vasa antibody from Santa Cruz
597 biologicals (anti rabbit 1:200), anti-Hts-1B1 from Developmental Studies Hybridoma
598 bank (anti-mouse 1:4 for serum, 1:40 for concentrate item), and anti-Fas3 from DSHB
599 (anti-mouse 1:50). We used the following secondary antibodies: Alexaflour 488, 568
600 (Invitrogen) at 1:500.

601

602 We performed immunostaining as described in Aruna et al. [38] and Flores et al. (Aruna
603 et al. 2009; Flores, Bubnell, et al. 2015). Briefly, we dissected ovaries and testes in ice-
604 cold 1X PBS and pipetted ovaries up and down to improve antibody permeability. We
605 fixed tissues in 4% paraformaldehyde, washed with PBST, blocked in PBTA (Alfa
606 Aesar, with 0.01% Triton X added), and then incubated in the appropriate primary
607 antibody in PBTA overnight. We then washed (PBST), blocked (PBTA), and incubated
608 the tissue in the appropriate secondary antibody for 2 hours, then washed (PBST) and
609 mounted in mounting media with DAPI (Vecta shield or Prolong Glass with NucBlue) for
610 imaging.

611

612 **Confocal Microscopy:**

613 We imaged ovaries and testes on a Zeiss i880 confocal microscope with 405nm, 488
614 nm, and 568 nm laser lines at 40X (Plan-Apochromat 1.4 NA, oil) (Cornell BRC Imaging
615 Core Facility). We analyzed and edited images using Fiji (ImageJ).

616

617 **RNA extraction:**

618 For RT-qPCR experiments we dissected ovaries from 10 one-day old females per
619 biological replicate or testes from 15 one-day old males in ice cold 1x PBS. The tissue
620 was immediately placed in NEB DNA/RNA stabilization buffer, homogenized with a
621 bead homogenizer, and then stored at -80°C until RNA extraction. We used the NEB
622 Total RNA mini-prep kit for all RNA extractions according to the manufacturer's
623 protocol and included the on column DNAse treatment. We assessed RNA
624 concentration and quality with a Qubit 4 fluorometer and a NanoDrop.
625
626 **RT-qPCR:**
627 For all RT-qPCR analyses, we used the Luna One Step RT-qPCR kit from NEB
628 according to the manufacturer's instructions at 10µl total volume in 384 well plates. We
629 used a Viia7 qPCR machine with the appropriate cycle settings as described in the
630 Luna One Step RT-qPCR kit.
631
632 For the analysis of *bam* expression in *D. ananassae*, we used primers to *D. ananassae*
633 *bam* with *D. ananassae Rp49* as a control (S1 Table). To assess the possibility that the
634 *bam* disruption allele induced exon skipping of the disrupted exon 1 in *D. teissieri*, we
635 designed a primer pair that spanned exon 1 to exon 2 and another pair that spanned
636 exon 2 to exon 3 (S1 Table). We used the exon 2 - exon 3 target as the control. For
637 both the *D. teissieri* and *D. ananassae* assays described above, we included a standard
638 curve for each target on every plate at a 1:2 dilution and then used the standard curve
639 method to calculate the relative quantity of *bam* (to either *Rp49* for *D. ananassae* or

640 *bam* exon 2-exon 3 for *D. teissieri*) with the QuantStudio software using the wildtype
641 *bam* genotype as a control for each species.
642
643 For the allele specific analysis in *D. teissieri,* we designed one primer pair specific to
644 the *bam* 3xP3-DsRed and 3xP3-YFP insertion alleles and another primer pair specific
645 to the wildtype allele. We then used these two targets to measure the relative
646 expression of the insertion allele to the wildtype allele in a single heterozygous sample.
647 The primer pair for the *bam* insertion alleles target the sequence between the SV40-
648 polyA tail of the 3xP3-DsRed and 3xP3-YFP insertion and the *bam* sequence
649 downstream of the insertion (S1 Table). The primer pair for the *bam* wildtype allele
650 target *bam* upstream and downstream of the 3xP3-DsRed and 3xP3-YFP insertion,
651 and therefore will not amplify the large insertion allele under RT-qPCR conditions (S1
652 Table). We included a standard curve for each target on every plate at a 1:2 dilution
653 and then used the standard curve method in the QuantStudio software to calculate the
654 Ct and Ct standard error for each target and each sample. We report the relative
655 quantity of the 3xP3-DsRed or 3xP3-YFP allele using the wildtype allele in the same
656 sample as a control by calculating $2^{-(\text{nullCt-wildtypeCt})}$.
657
658 **Genomic analysis of *bam* copy number in *D. teissieri:***
659 While *bam* is reported as a 1:1 syntenic ortholog on FlyBase for *D. melanogaster, D.*
660 *simulans, D. yakuba,* and *D. ananassae,* data for *D. teissieri* is not available. To ask if
661 *bam* has been recently duplicated in *D. teissieri,* we generated a blast database (blastn
662 v 2.9.0) from a new de novo assembled *D. teissieri* reference genome (accession

663 GCA_016746235.1) and blasted *D. teissieri bam* from the resequencing described
664 above.
665
666 Additionally, to assess read coverage for *bam* compared to the surrounding loci and the
667 entire chromosome 3R, we used publicly available short read WGS data for *D. teissieri*
668 (SRR13202235) and used bwa-mem (v 0.7.17) to map reads to a new de novo
669 assembled *D. yakuba* reference genome (accession GCA_016746365.1). We visualized
670 the alignment and assessed read coverage using Geneious.
671
672 **Population genetic analyses:**
673 **Population samples:**
674 The *D. yakuba*, *D. santomea*, and *D. teissieri* population sample lines were gifted by
675 Brandon Cooper and Daniel Matute (Cooper et al. 2017). The *D. yakuba* and *D. teissieri*
676 lines were collected in Bioko in 2013, the *D. santomea* sample was collected in Sao
677 Tome in 2015. The *D. affinis* population sample lines were gifted by Robert Unckless
678 (S2 Table). The *D. mojavensis* population sample is from Organ Pipe National
679 Monument, Arizona and DNA from this sample was gifted by Erin Kelleher and Luciano
680 Matzkin. The *D. pseudoobscura* population sample is from Apple Hill, California, as
681 described in (Schaeffer and Miller 1991). We used previously prepared DNA from the *D.*
682 *pseudoobscura* population sample as described in (Schaeffer and Miller 1991).
683
684 **Resequencing:**

685 We prepared genomic DNA from *D. affinis, D. yakuba*, *D. santomea*, and *D. teissieri*
686 samples using the Qiagen PureGene kit. We used Primer3 to generate primers to
687 amplify *bam* from *D. affinis, D. mojavensis, D. pseudoobscura, D. yakuba*, *D. santomea*,
688 and *D. teissieri* population samples (S7 Table). We used existing polymorphism data
689 (Daniel Matute, personal communication) to generate primers for *D. yakuba*, *D.*
690 *santomea*, and *D. teissieri*. We resequenced *bam* using Sanger sequencing from
691 5'UTR-3'UTR for *D. yakuba*, *D. santomea*, and *D. teissieri* and *bam* exons and introns
692 for *D. affinis* (Cornell BRC Genomics Facility). We used Geneious for aligning the
693 sequences and calling polymorphisms. We generated fasta files for each individual. We
694 used DnaSP to phase individuals with heterozygous sites, and then randomly picked
695 one allele for further analyses (Bauer DuMont et al. 2007). We will deposit all
696 resequencing data described here in Genbank.
697
698 **Existing polymorphism data:**
699 We used polymorphism data for *D. melanogaster* from the Zambia population sample
700 from the Drosophila genome Nexus (Lack et al. 2015), as this is the largest population
701 sample with intact *bam* sequence and represents a population in the *D. melanogaster*
702 ancestral range. We used polymorphism data for *D. simulans* from the California
703 population sample (Signor et al. 2018). For the *D. melanogaster* Zambia population
704 sample, we removed a single individual that contained missing nucleotide calls in the
705 *bam* coding sequence (ZI117). As we filtered polymorphisms at < 5% frequency,
706 omitting this single individual would not affect our downstream analyses. In the *D.*
707 *simulans* CA population sample there were no individuals with missing data.

708

709 *D. ananassae bam* polymorphism, and single *D. atripex, D. bipectinata bam* sequences
710 are from Choi et al. (Choi and Aquadro 2014). We obtained single *bam* sequences for
711 species used for outgroups from FlyBase (*D. erecta*), and Genbank (*D. eugracilis, D.*
712 *arizonae, D. navojoa, D. miranda, D. subobscura).*

713

714 **Alignments and ancestral sequence reconstruction:**

715 We performed all multiple sequence alignments for the *bam* coding sequences using
716 PRANK (v.170427) with the -codon and -F parameters and using the PRANK generated
717 guide tree. As *bam* is highly divergent across the *Drosophila* genus, we generated
718 multiple sequence alignments only among closely related clusters of species to ensure
719 alignment quality. We generated a multiple sequence alignment of the *melanogaster*
720 subgroup species (*D. melanogaster, D. simulans, D. yakuba, D. santomea, D. teissieri,*
721 *D. erecta, D. eugracilis*), a multiple sequence alignment of *D. ananassae, D. atripex,*
722 and *D. bipectinata*, a multiple sequence alignment of *D. mojavensis, D. arizonae, and D.*
723 *navajo*, and a multiple sequence alignment of *D. affinis, D. pseudoobscura, D. miranda,*
724 and *D. subobscura*.

725

726 We used only unique sequences for input to codeml. We used the codeml package from
727 PAML (v. 4.9) (Yang 1997; Yang 2007) to generate the predicted common ancestor
728 sequences to calculate lineage-specific divergence for *bam* with the McDonald-
729 Kreitman test. We used the PRANK alignments and their corresponding gene trees as
730 input to codeml with the following control file parameters (noisy = 9, verbose = 2,

731 runmode = 0, seqtype = 1, CodonFreq = 2, clock = 0, aaDist = 0, model = 0, NSsites =
732 0, icode = 0, getSE = 0, RateAncestor = 1, Small_Diff = .5e-6, cleandata = 0, method =
733 1).
734
735 We used the http://mkt.uab.cat/mkt/mkt.asp webtool to perform the standard McDonald-
736 Kreitman test (MKT) comparing nonsynonymous vs. synonymous changes (Egea et al.
737 2008). We excluded polymorphic sites at < 5% frequency, as these are likely slightly
738 deleterious alleles that have not yet been purged by purifying selection (Charlesworth
739 and Eyre-Walker 2008). For each species where we had polymorphism data, we
740 performed the MKT using the specified predicted common ancestral sequence to
741 calculate lineage-specific divergence. We report the values of the contingency table, the
742 P-value of the Chi-Square test, as well as alpha, the proportion of fixations predicted to
743 be due to positive selection (Eyre-Walker 2006).
744

745 **Acknowledgements:**

746 We thank Santiago Herrera Alvarez for resequencing *bam* from *D. affinis* and Jae
747 Young Choi for resequencing *bam* from *D. pseudoobscura* and *D. mojavensis.* We
748 thank Daniel Matute, Brandon Cooper, Robert Unckless, Erin Kelleher, and Luciano
749 Matzkin for the population samples they provided for this study. Additionally, we thank
750 David L. Stern for his advice and guidance in designing the *bam* null alleles and for an
751 extremely thoughtful and critical review of an earlier draft of the manuscript. We are
752 grateful to Mariana F. Wolfner, Andrew G. Clark, Miwa Wenzel and Catherine

Kagemann for valuable input and discussion of these experiments and results and helpful comments on this manuscript.

Data Availability:

Sequence data generated in this study will be deposited in GenBank prior to publication. The remaining data underlying this article are available in the article and in its online supplementary material. Fly lines, CRISPR/Cas9 reagents, and plasmids used in this study are available upon request.

Funding:

This work was supported by National Institutes of Health grant R01-GM095793 to C.F.A. and by the National Science Foundation Graduate Research Fellowship Program DGE-114415 to J.E.B.

769 REFERENCES

770 Akashi H. 1999. Inferring the fitness effects of DNA mutations from polymorphism and
771 divergence data: Statistical power to detect directional selection under stationarity
772 and free recombination. Genetics. 151(1). doi:10.1093/genetics/151.1.221.
773 Aquadro CF, Lado KM, Noon WA. 1988. The rosy region of Drosophila melanogaster
774 and Drosophila simulans. I. Contrasting levels of naturally occurring DNA restriction
775 map variation and divergence. Genetics. 119(4):875–888.
776 doi:10.1093/genetics/119.4.875.
777 Aravin AA, Hannon GJ, Brennecke J. 2007. The Piwi-piRNA pathway provides an
778 adaptive defense in the transposon arms race. Science (80-). 318(5851).
779 doi:10.1126/science.1146484.
780 Aruna S, Flores HA, Barbash DA. 2009. Reduced fertility of Drosophila melanogaster
781 Hybrid male rescue (Hmr) mutant females is partially complemented by Hmr
782 orthologs from sibling species. Genetics. doi:10.1534/genetics.108.100057.
783 Bauer DuMont VL, Flores HA, Wright MH, Aquadro CF. 2007. Recurrent positive
784 selection at Bgcn, a key determinant of germ line differentiation, does not appear to
785 be driven by simple coevolution with its partner protein bam. Mol Biol Evol.
786 24(1):182–191. doi:10.1093/molbev/msl141.
787 Blondel L, Jones TEM, Extavour CG. 2020. Bacterial contribution to genesis of the
788 novel germ line determinant Oskar. Elife. doi:10.7554/eLife.45539.
789 Brogna S, Wen J. 2009. Nonsense-mediated mRNA decay (NMD) mechanisms. Nat
790 Struct Mol Biol. doi:10.1038/nsmb.1550.
791 Bubnell JE, Fernandez-Begne P, Ulbing CKS, Aquadro CF. 2021. Diverse w Mel

792 variants of Wolbachia pipientis differentially rescue fertility and cytological defects
793 of the bag of marbles partial loss of function mutation in Drosophila melanogaster .
794 G3 Genes|Genomes|Genetics. doi:10.1093/g3journal/jkab312.
795 Cariou M, Duret L, Charlat S. 2017. The global impact of Wolbachia on mitochondrial
796 diversity and evolution. J Evol Biol. doi:10.1111/jeb.13186.
797 Charlesworth J, Eyre-Walker A. 2008. The McDonald-Kreitman test and slightly
798 deleterious mutations. Mol Biol Evol. doi:10.1093/molbev/msn005.
799 Chen D, McKearin D. 2003. Dpp Signaling Silences bam Transcription Directly to
800 Establish Asymmetric Divisions of Germline Stem Cells. Curr Biol. 13(20):1786–
801 1791. doi:10.1016/j.cub.2003.09.033.
802 Chen D, Tang JX, Li B, Hou L, Wang X, Kang L. 2018. CRISPR/Cas9-mediated
803 genome editing induces exon skipping by complete or stochastic altering splicing in
804 the migratory locust. BMC Biotechnol. doi:10.1186/s12896-018-0465-7.
805 Chen D, Wu C, Zhao S, Geng Q, Gao Y, Li X, Zhang Y, Wang Z. 2014. Three RNA
806 Binding Proteins Form a Complex to Promote Differentiation of Germline Stem Cell
807 Lineage in Drosophila. PLoS Genet. 10(11):e1004797.
808 doi:10.1371/journal.pgen.1004797.
809 Chen S, Zhang YE, Long M. 2010. New Genes in Drosophila Quickly Become
810 Essential. Science (80-). 330(6011):1682–1685. doi:10.1126/science.1196380.
811 Choi JY, Aquadro CF. 2014. The coevolutionary period of Wolbachia pipientis infecting
812 Drosophila ananassae and its impact on the evolution of the host germline stem
813 cell regulating genes. Mol Biol Evol. doi:10.1093/molbev/msu204.
814 Choi JY, Aquadro CF. 2015. Molecular evolution of drosophila germline stem cell and

815 neural stem cell regulating genes. Genome Biol Evol. 7(11):3097–3114.
816 doi:10.1093/gbe/evv207.
817 Civetta A, Rajakumar SA, Brouwers B, Bacik JP. 2006. Rapid evolution and gene-
818 specific patterns of selection for three genes of spermatogenesis in Drosophila. Mol
819 Biol Evol. 23(3):655–662. doi:10.1093/molbev/msj074.
820 Clark AG, Eisen MB, Smith DR, Bergman CM, Oliver B, Markow TA, Kaufman TC,
821 Kellis M, Gelbart W, Iyer VN, et al. 2007. Evolution of genes and genomes on the
822 Drosophila phylogeny. Nature. doi:10.1038/nature06341.
823 Cooper BS, Ginsberg PS, Turelli M, Matute DR. 2017. Wolbachia in the Drosophila
824 yakuba complex: Pervasive frequency variation and weak cytoplasmic
825 incompatibility, but no apparent effect on reproductive isolation. Genetics.
826 205(1):333–351. doi:10.1534/genetics.116.196238.
827 Egea R, Casillas S, Barbadilla A. 2008. Standard and generalized McDonald-Kreitman
828 test: a website to detect selection by comparing different classes of DNA sites.
829 Nucleic Acids Res. doi:10.1093/nar/gkn337.
830 Eyre-Walker A. 2006. The genomic rate of adaptive evolution. Trends Ecol Evol.
831 doi:10.1016/j.tree.2006.06.015.
832 Findlay GD, MacCoss MJ, Swanson WJ. 2009. Proteomic discovery of previously
833 unannotated, rapidly evolving seminal fluid genes in Drosophila. Genome Res.
834 19(5):886–896. doi:10.1101/gr.089391.108.
835 Flores HA, Bubnell JE, Aquadro CF, Barbash DA. 2015. The Drosophila bag of marbles
836 Gene Interacts Genetically with Wolbachia and Shows Female-Specific Effects of
837 Divergence. PLoS Genet. 11(8):e1005453. doi:10.1371/journal.pgen.1005453.

838 Flores HA, DuMont VLB, Fatoo A, Hubbard D, Hijji M, Barbash DA, Aquadro CF. 2015.
839 Adaptive evolution of genes involved in the regulation of germline stem cells in
840 Drosophila melanogaster and D. simulans. G3 Genes, Genomes, Genet. 5(4):583–
841 592. doi:10.1534/g3.114.015875.
842 Gleason RJ, Anand A, Kai T, Chen X. 2018. Protecting and diversifying the germline.
843 Genetics. 208(2):435–471. doi:10.1534/genetics.117.300208.
844 Glover DM, Raff J, Karr TL, O'Neill SL, Lin H, Wolfner MF. 1990. Parasites in
845 Drosophila embryos. Nature. 348:117. doi:10.1038/348117a0.
846 Gönczy P, Matunis E, DiNardo S. 1997. bag-of-marbles and benign genial cell
847 neoplasm act in the germline to restrict proliferation during Drosophila
848 spermatogenesis. Development. 124(21):4361–4371.
849 doi:10.1242/dev.124.21.4361.
850 Gratz SJ, Ukken FP, Rubinstein CD, Thiede G, Donohue LK, Cummings AM, Oconnor-
851 Giles KM. 2014. Highly specific and efficient CRISPR/Cas9-catalyzed homology-
852 directed repair in Drosophila. Genetics. 196(4):961–971.
853 doi:10.1534/genetics.113.160713.
854 Gubala AM, Schmitz JF, Kearns MJ, Vinh TT, Bornberg-Bauer E, Wolfner MF, Findlay
855 GD. 2017. The Goddard and Saturn Genes Are Essential for Drosophila Male
856 Fertility and May Have Arisen de Novo. Mol Biol Evol. doi:10.1093/molbev/msx057.
857 Hinnant TD, Merkle JA, Ables ET. 2020. Coordinating Proliferation, Polarity, and Cell
858 Fate in the Drosophila Female Germline. Front Cell Dev Biol. 8:19.
859 doi:10.3389/fcell.2020.00019.
860 Ho J, Tumkaya T, Aryal S, Choi H, Claridge-Chang A. 2019. Moving beyond P values:

861 data analysis with estimation graphics. Nat Methods. 16(7):565–566.
862 doi:10.1038/s41592-019-0470-3.
863 Hoffmann AA, Turelli M, Simmons GM. 1986. Unidirectional incompatibility between
864 populations of Drosophila simulans. Evolution (N Y). doi:10.1111/j.1558-
865 5646.1986.tb00531.x.
866 Howe KL, Contreras-Moreira B, De Silva N, Maslen G, Akanni W, Allen J, Alvarez-
867 Jarreta J, Barba M, Bolser DM, Cambell L, et al. 2020. Ensembl Genomes 2020-
868 enabling non-vertebrate genomic research. Nucleic Acids Res. 48(D1).
869 doi:10.1093/nar/gkz890.
870 Insco ML, Bailey AS, Kim J, Olivares GH, Wapinski OL, Tam CH, Fuller MT. 2012. A
871 self-limiting switch based on translational control regulates the transition from
872 proliferation to differentiation in an adult stem cell lineage. Cell Stem Cell.
873 11(5):689–700. doi:10.1016/j.stem.2012.08.012.
874 Insco ML, Leon A, Tam CH, McKearin DM, Fuller MT. 2009. Accumulation of a
875 differentiation regulator specifies transit amplifying division number in an adult stem
876 cell lineage. Proc Natl Acad Sci. 106(52):22311–22316.
877 doi:10.1073/PNAS.0912454106.
878 Jenny A, Hachet O, Závorszky P, Cyrklaff A, Weston MDJ, St Johnston D, Erdélyi M,
879 Ephrussi A. 2006. A translation-independent role of oskar RNA in early Drosophila
880 oogenesis. Development. 133(15):2827–2833. doi:10.1242/dev.02456.
881 Jiang X, Assis R. 2017. Natural selection drives rapid functional evolution of young
882 drosophila duplicate genes. Mol Biol Evol. 34(12):3089–3098.
883 doi:10.1093/molbev/msx230.

884 Kaessmann H. 2010. Origins, evolution, and phenotypic impact of new genes. Genome
885 Res. 20(10):1313–1326. doi:10.1101/gr.101386.109.
886 Kahney EW, Snedeker JC, Chen X. 2019. Regulation of Drosophila germline stem cells.
887 Curr Opin Cell Biol. 60:27–35. doi:10.1016/j.ceb.2019.03.008.
888 Kelleher ES, Jaweria J, Akoma U, Ortega L, Tang W. 2018. QTL mapping of natural
889 variation reveals that the developmental regulator bruno reduces tolerance to P-
890 element transposition in the Drosophila female germline. PLoS Biol. 16(10).
891 doi:10.1371/journal.pbio.2006040.
892 Klasberg S, Bitard-Feildel T, Callebaut I, Bornberg-Bauer E. 2018. Origins and
893 structural properties of novel and *de novo* protein domains during insect evolution.
894 FEBS J. 285(14):2605–2625. doi:10.1111/febs.14504.
895 Kriventseva E V., Kuznetsov D, Tegenfeldt F, Manni M, Dias R, Simão FA, Zdobnov
896 EM. 2019. OrthoDB v10: Sampling the diversity of animal, plant, fungal, protist,
897 bacterial and viral genomes for evolutionary and functional annotations of
898 orthologs. Nucleic Acids Res. 47(D1). doi:10.1093/nar/gky1053.
899 Lack JB, Cardeno CM, Crepeau MW, Taylor W, Corbett-Detig RB, Stevens KA, Langley
900 CH, Pool JE. 2015. The drosophila genome nexus: A population genomic resource
901 of 623 Drosophila melanogaster genomes, including 197 from a single ancestral
902 range population. Genetics. doi:10.1534/genetics.115.174664.
903 Lavoie CA, Ohlstein B, McKearin DM. 1999. Localization and function of bam protein
904 require the benign gonial cell neoplasm gene product. Dev Biol.
905 doi:10.1006/dbio.1999.9346.
906 Levine MT, Jones CD, Kern AD, Lindfors HA, Begun DJ. 2006. Novel genes derived

907 from noncoding DNA in Drosophila melanogaster are frequently X-linked and
908 exhibit testis-biased expression. National Academy of Sciences.
909 Li Y, Minor NT, Park JK, McKearin DM, Maines JZ. 2009. Bam and Bgcn antagonize
910 Nanos-dependent germ-line stem cell maintenance. Proc Natl Acad Sci U S A.
911 106(23):9304–9309. doi:10.1073/pnas.0901452106.
912 McKearin DM, Spradling AC. 1990. Bag-of-marbles: A Drosophila gene required to
913 initiate both male and female gametogenesis. Genes Dev. 4(12 B):2242–2251.
914 doi:10.1101/gad.4.12b.2242.
915 Messer PW, Petrov DA. 2013. Frequent adaptation and the McDonald-Kreitman test.
916 Proc Natl Acad Sci U S A. 110(21):8615–8620. doi:10.1073/pnas.1220835110.
917 Mou H, Smith JL, Peng L, Yin H, Moore J, Zhang XO, Song CQ, Sheel A, Wu Q, Ozata
918 DM, et al. 2017. CRISPR/Cas9-mediated genome editing induces exon skipping by
919 alternative splicing or exon deletion. Genome Biol. 18(1):108. doi:10.1186/s13059-
920 017-1237-8.
921 Pereverzev AP, Gurskaya NG, Ermakova G V., Kudryavtseva EI, Markina NM, Kotlobay
922 AA, Lukyanov SA, Zaraisky AG, Lukyanov KA. 2015. Method for quantitative
923 analysis of nonsense-mediated mRNA decay at the single cell level. Sci Rep.
924 5(1):1–10. doi:10.1038/srep07729.
925 Port F, Chen HM, Lee T, Bullock SL. 2014. Optimized CRISPR/Cas tools for efficient
926 germline and somatic genome engineering in Drosophila. Proc Natl Acad Sci U S
927 A. 111(29). doi:10.1073/pnas.1405500111.
928 Schaeffer SW, Miller EL. 1991. Nucleotide sequence analysis of Adh genes estimates
929 the time of geographic isolation of the Bogota population of Drosophila

930 pseudoobscura. Proc Natl Acad Sci U S A. 88(14):6097–6101.
931 doi:10.1073/pnas.88.14.6097.
932 Shivdasani AA, Ingham PW. 2003. Regulation of Stem Cell Maintenance and Transit
933 Amplifying Cell Proliferation by TGF-β Signaling in Drosophila Spermatogenesis.
934 Curr Biol. doi:10.1016/j.cub.2003.10.063.
935 Siddiq MA, Loehlin DW, Montooth KL, Thornton JW. 2017. Experimental test and
936 refutation of a classic case of molecular adaptation in Drosophila melanogaster.
937 Nat Ecol Evol. 1(2). doi:10.1038/s41559-016-0025.
938 Signor SA, New FN, Nuzhdin S. 2018. A large panel of drosophila simulans reveals an
939 abundance of common variants. Genome Biol Evol. doi:10.1093/gbe/evx262.
940 Simkin A, Wong A, Poh YP, Theurkauf WE, Jensen JD. 2013. Recurrent and recent
941 selective sweeps in the piRNA pathway. Evolution (N Y). 67(4):1081–1090.
942 doi:10.1111/evo.12011.
943 Sui T, Song Y, Liu Z, Chen M, Deng J, Xu Y, Lai L, Li Z. 2018. CRISPR-induced exon
944 skipping is dependent on premature termination codon mutations. Genome Biol.
945 doi:10.1186/s13059-018-1532-z.
946 Thurmond J, Goodman JL, Strelets VB, Attrill H, Gramates LS, Marygold SJ, Matthews
947 BB, Millburn G, Antonazzo G, Trovisco V, et al. 2019. FlyBase 2.0: the next
948 generation. Nucleic Acids Res. 47(D1):D759–D765. doi:10.1093/NAR/GKY1003.
949 Ting X. 2013. Control of germline stem cell self-renewal and differentiation in the
950 Drosophila ovary: Concerted actions of niche signals and intrinsic factors. Wiley
951 Interdiscip Rev Dev Biol. 2(2):261–273. doi:10.1002/wdev.60.
952 True JR, Haag ES. 2001. Developmental system drift and flexibility in evolutionary

953 trajectories. Evol Dev. 3(2):109–119. doi:10.1046/j.1525-142X.2001.003002109.x.
954 Turissini DA, Liu G, David JR, Matute DR. 2015. The evolution of reproductive isolation
955 in the Drosophila yakuba complex of species. J Evol Biol. 28(3):557–575.
956 doi:10.1111/jeb.12588.
957 Vakirlis N, McLysaght A. 2019. Computational Prediction of De Novo Emerged Protein-
958 Coding Genes. In: Methods in Molecular Biology. Vol. 1851. Humana Press Inc. p.
959 63–81.
960 Werren JH, Baldo L, Clark ME. 2008. Wolbachia: Master manipulators of invertebrate
961 biology. Nat Rev Microbiol. 6(10):741–751. doi:10.1038/nrmicro1969.
962 Wilson BA, Foy SG, Neme R, Masel J. 2017. Young genes are highly disordered as
963 predicted by the preadaptation hypothesis of de novo gene birth. Nat Ecol Evol.
964 1(6). doi:10.1038/s41559-017-0146.
965 Witt E, Benjamin S, Svetec N, Zhao L. 2019. Testis single-cell RNA-seq reveals the
966 dynamics of de novo gene transcription and germline mutational bias in drosophila.
967 Elife. doi:10.7554/eLife.47138.
968 Yang Z. 1997. Paml: A program package for phylogenetic analysis by maximum
969 likelihood. Bioinformatics. doi:10.1093/bioinformatics/13.5.555.
970 Yang Z. 2007. PAML 4: Phylogenetic analysis by maximum likelihood. Mol Biol Evol.
971 doi:10.1093/molbev/msm088.
972 Zhai W, Nielsen R, Slatkin M. 2009. An investigation of the statistical power of neutrality
973 tests based on comparative and population genetic data. Mol Biol Evol. 26(2).
974 doi:10.1093/molbev/msn231.
975 Zhou Q, Zhang G, Zhang Y, Xu S, Zhao R, Zhan Z, Li X, Ding Y, Yang S, Wang W.

976 2008. On the origin of new genes in Drosophila. Genome Res. 18(9):1446–1455.
977 doi:10.1101/gr.076588.108.
978
979

Fig 1. Species chosen to generate *bam* null alleles using CRISPR/Cas9 to disrupt *bam* with a trackable eye marker cassette. (A) The five species we chose to generate *bam* null alleles span approximately 15 million years of divergence and show different patterns of evolution at *bam* as previously described (Civetta et al. 2006; Bauer DuMont et al. 2007; Choi and Aquadro 2014). Prior to this study, evidence of positive selection has been reported for lineages in red (Civetta et al. 2006; Bauer DuMont et al. 2007), no evidence of positive selection has been reported for lineages in blue (Choi and Aquadro 2014), and lineages in black have not yet been tested. (B) Schematic for generating null alleles with trackable eye markers using CRISPR/Cas9. We generate two null alleles using different color eye markers and cross the heterozygotes together to generate an easily trackable null genotype.

Fig 2. *Bam* is necessary for female and male fertility in *D. melanogaster, D. simulans, and D. yakuba,* but not for *D. ananassae* males nor both *D. teissieri* males and females. Swarm plots showing the total progeny per female or per male for each *bam* genotype. Dotted boxes show genotypes where the phenotype did not match that of *D. melanogaster.* For *D. melanogaster, D. simulans, and D. yakuba*, the *bam* null DsRed/YFP females and males were sterile ($P < 0.0001$, permutation test), and the heterozygous genotypes did not have a significant effect on fertility ($P > 0.05$, permutation test). For *D. teissieri,* the *bam* null DsRed/YFP females and males did not have significantly different fertility from wildtype, nor did the heterozygotes. For *D. ananassae*, the *bam* null DsRed/YFP females were sterile ($P < 0.0001$, permutation test), and the heterozygotes did not affect fertility. However, the *bam* null DsRed/YFP males were fertile and there was no significant difference between the null and heterozygotes and wildtype fertility ($P>0.05$, permutation test).

Fig 3. *Bam* is necessary for female and male germline stem cell differentiation in *D. melanogaster, D. simulans, and D. yakuba,* but not for *D. ananassae* males nor *D. teissieri* males and females. (A) Schematics of ovaries and testes showing the *bam* wildtype and null cytological phenotypes in *D. melanogaster*. Wildtype *bam* ovaries exhibit developing egg chambers with differentiated nurse cells and testes exhibit large

differentiated spermatocytes. Null *bam* ovaries exhibit egg chambers filled with small GSC-like tumors that contain undeveloped fusomes and testes exhibit cysts filled with small over-proliferating spermatogonia. (B) Ovaries and testes from all five species of wildtype (*bam*$^{+}$/*bam*$^{+}$*),* heterozygous (YFP/+ or DsRed/+)*,* and null (DsRed/YFP) *bam* genotypes. All tissue is labeled with antibodies to Vasa (germline) and Hts-1B1 (fusome). Dashed boxes indicate genotypes and tissue that are not consistent with the *D. melanogaster* phenotype. Ovaries and testes from all five species exhibit developing nurse cells or spermatocytes (respectively) for wildtype and heterozygous *bam* genotypes. We did not observe any tumorous cysts (arrowheads). Ovaries and testes from *bam* null *D. melanogaster, D. simulans, and D. yakuba* all exhibited cysts filled with GSC-like tumors (ovaries) or over-proliferating spermatogonia (testes) (arrows). The *bam* null ovaries exhibit undeveloped fusomes. *D. ananassae bam* null ovaries exhibited the tumorous egg chamber phenotype (arrow), however testes exhibited large developing spermatocytes (arrowhead) and we did not observe any tumors. The *bam* null *D. teissieri* ovaries and testes exhibited nurse cell positive egg chambers and developing spermatocytes (respectively) (arrowheads) and we did not observe any tumors.

Fig 4. Loss of *bam* function in *D. ananassae* males shows mis-expression of Fas3, a marker expressed in the hub. All testes tissue is labeled with antibodies for Vasa (germline) and Fas3 (hub, arrowheads). (A) *D. melanogaster bam* wildtype testes with Fas3 expression limited to the hub (inset) and featuring large differentiating spermatogonia. (B) *D. melanogaster bam* null testes feature ectopic Fas3 expression and small over-proliferating spermatogonia. (C) *D. ananassae bam* wildtype testes with Fas3 expression limited to the hub and featuring large differentiating spermatogonia. (D) *D. ananassae bam* null testes with ectopic Fas3 expression and large differentiating spermatogonia.

Fig 5. *Bam* shows lineage-specific signals of positive selection within the melanogaster species subgroup and no evidence of positive selection outside of

the melanogaster species subgroup. Cladogram of *Drosophila* species we sampled in this study or previously published. Red lineages represent lineages where we have evidence of positive selection at *bam* with the McDonald Kreitman test. Blue lineages are lineages of which we could not reject neutrality with the McDonald Kreitman test. The 2X2 table from the McDonald Kreitman test is shown on the right (N = nonsynonymous, S = synonymous). Alpha is the proportion of nonsynonymous fixations predicted to be due to positive selection. p-value is from the chi-sq test, n is sample size. [1] *2X2 table and statistics from Bauer DuMont et al. 2007 [2]polymorphism data from Choi and Aquadro 2014.

Fig S1. Extended plots from Fig 3 including the Cumming estimation plot below the swarm plot. *bam* is necessary for female and male fertility in *D. melanogaster, D. simulans, and D. yakuba,* but not for *D. ananassae* males nor both *D. teissieri* males and females. The Cumming estimation plot displays the 95% confidence interval effect size. As stated in Fig 3*, D. melanogaster, D. simulans, and D. yakuba*, the *bam* null DsRed/YFP females and males were sterile ($P < 0.0001$, permutation test), and the heterozygous genotypes did not have a significant effect on fertility ($P > 0.05$, permutation test). For *D. teissieri,* the *bam* null DsRed/YFP females and males did not have significantly different fertility from wildtype, nor did the heterozygotes. For *D. ananassae*, the *bam* null DsRed/YFP females were sterile ($P < 0.0001$, permutation test), and the heterozygotes did not affect fertility. However, the *bam* null DsRed/YFP males were fertile and there was no significant difference between the null and heterozygotes and wildtype fertility ($P>0.05$, permutation test)

Fig S2. RT-qPCR experiment to assess *bam* mRNA in *D. ananassae bam* null genotypes reported as the relative quantity (RQ) of *bam* expression to the housekeeping control RP49. *bam* expression in testes of the null (DsRed/YFP) genotype is significantly reduced (standard error) relative to *bam* expression in testes of the wildtype genotype at approximately 10%, consistent with expectations for NMD. The

heterozygous genotypes DsRed/+ and YFP/+ do not show reduced *bam* expression relative to wildtype.

Fig S3. RT-qPCR experiment to detect patterns consistent with nonsense mediated mRNA decay of the *bam* disruption allele in *D. teissieri* reported as the relative quantity (RQ) of mRNA from the *bam* disruption allele to the *bam* wildtype allele in heterozygotes. Significance reported as standard error (A) Expression of the *bam* null allele relative to the *bam* wildtype allele in ovaries. Both heterozygous genotypes DsRed/+ and YFP/+ show less than 10% of expression of the *bam* null allele relative to the wildtype allele, consistent with expectations for NMD. The wildtype negative control shows little to no expression of the null allele as expected. (B) Expression of the *bam* null allele relative to the *bam* wildtype allele in testes. Both heterozygous genotypes DsRed/+ and YFP/+ show less than 50% of expression of the *bam* null allele relative to the wildtype allele, consistent with expectations for NMD. The wildtype negative control shows little to no expression of the null allele as expected.

Fig S4. RT-qPCR experiment to detect evidence of exon skipping of the exon containing the *bam* disruption reported as the relative quantity (RQ) of *bam* exon 1 to exon 2. Significance reported as standard error (A) Expression of *bam* exon 1 relative to exon 2 in ovaries. The RQ of exon 1 to exon 2 in the *bam* null DsRed/YFP genotype is not significantly different than the RQ of exon 1 to exon 2 in the *bam* wildtype genotype, indicating that expression of the exon containing the disruption is comparable to the unaffected exon in both the null and wildtype genotype, and therefore exon skipping is not likely occurring in females. (B) Expression of *bam* exon 1 relative to exon 2 in testes. The RQ of exon 1 to exon 2 in the *bam* null DsRed/YFP genotype is not significantly different than the RQ of exon 1 to exon 2 in the *bam* wildtype genotype, indicating that expression of the exon containing the disruption is comparable to the unaffected exon in both the null and wildtype genotype, and therefore exon skipping is not likely occurring in males.

Table 1. Abbreviations for *bam* genotypes for all species and the expected phenotypes as observed in *D. melanogaster*.

		***D. melanogaster* Phenotype Expectations**		
Genotype	**Abbreviation**	**Eye Color**	**Fertility**	**Cytological**
bam^{+}/bam^{+}	wildtype	white	wildtype	wildtype
$bam^{3xP3\text{-}DsRed}/bam^{+}$	DsRed/+	DsRed	wildtype	wildtype
$bam^{3xP3\text{-}YFP}/bam^{+}$	YFP/+	YFP	wildtype	wildtype
$bam^{3xP3\text{-}DsRed}/bam^{3xP3\text{-}YFP}$	DsRed/YFP	DsRed & YFP	sterile	tumorous ovaries and testes

Fig1

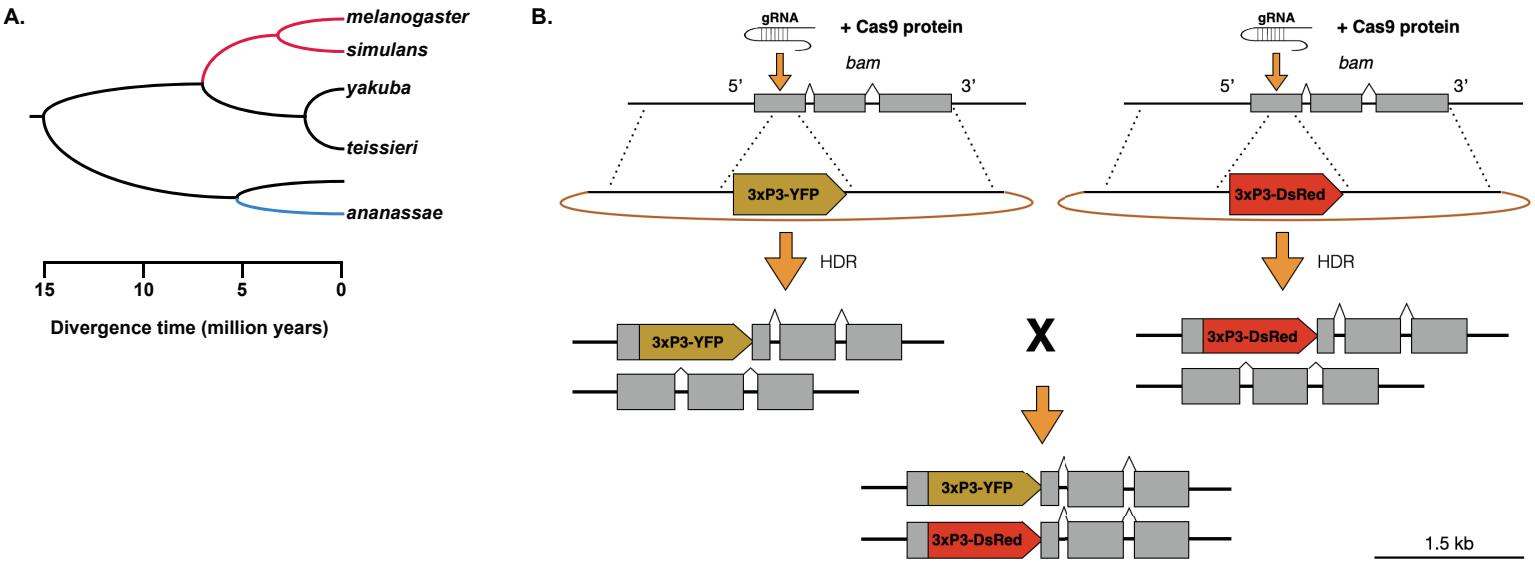
A.
melanogaster
simulans
yakuba
teissieri
ananassae
15
10
5
0
Divergence time (million years)
B.
gRNA
+ Cas9 protein
bam
5'
3'
3xP3-YFP
HDR
gRNA
+ Cas9 protein
bam
5'
3'
3xP3-DsRed
HDR
3xP3-YFP
X
3xP3-DsRed
3xP3-YFP
3xP3-DsRed
1.5 kb

Fig2

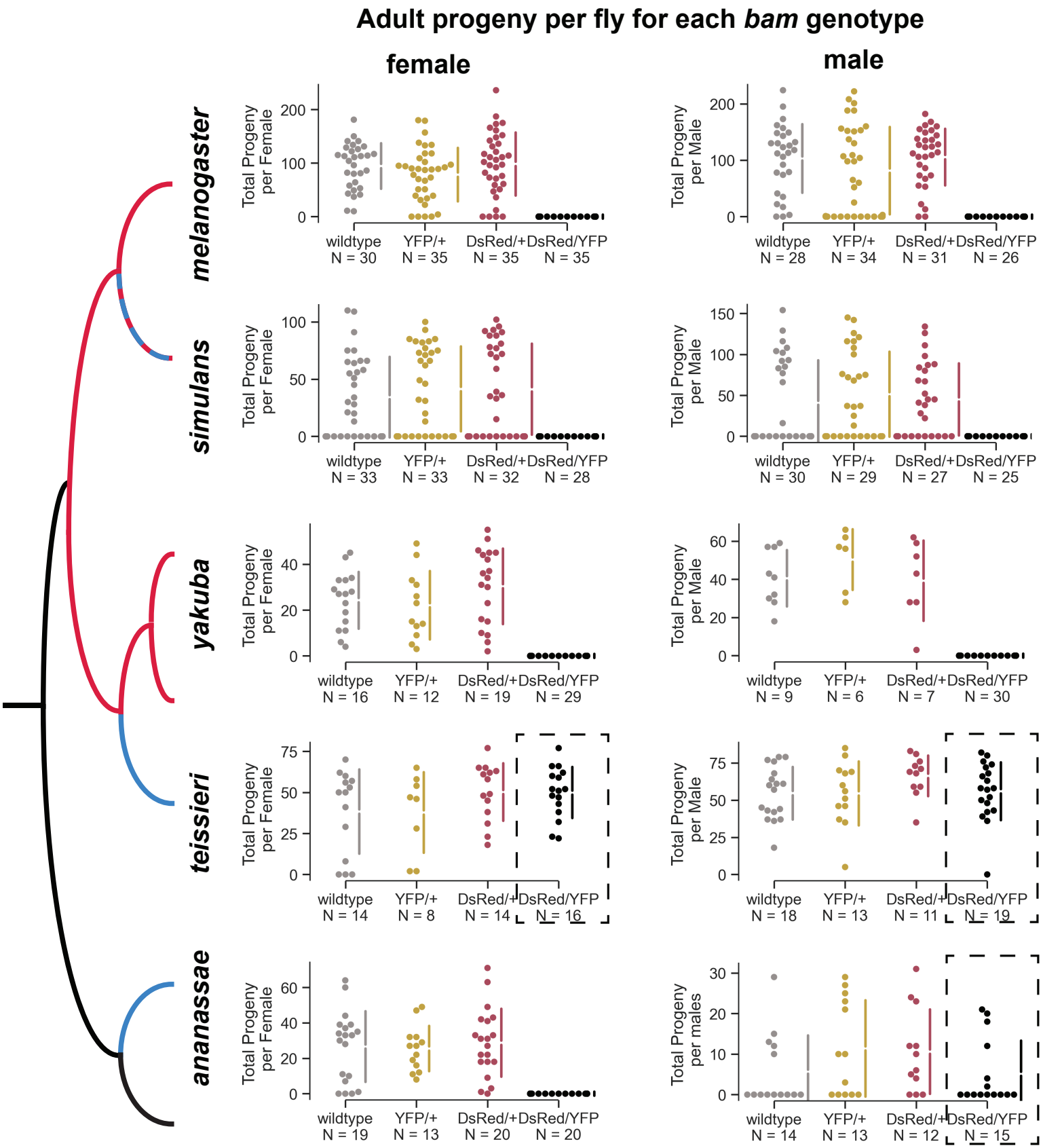
Adult progeny per fly for each bam genotype
female
male
melanogaster
simulans
yakuba
teissieri
ananassae
Total Progeny per Female
Total Progeny per Male
Total Progeny per males
wildtype
YFP/+
DsRed/+
DsRed/YFP
N = 30
N = 35
N = 35
N = 35
N = 28
N = 34
N = 31
N = 26
N = 33
N = 33
N = 32
N = 28
N = 30
N = 29
N = 27
N = 25
N = 16
N = 12
N = 19
N = 29
N = 9
N = 6
N = 7
N = 30
N = 14
N = 8
N = 14
N = 16
N = 18
N = 13
N = 11
N = 19
N = 19
N = 13
N = 20
N = 20
N = 14
N = 13
N = 12
N = 15

Fig3

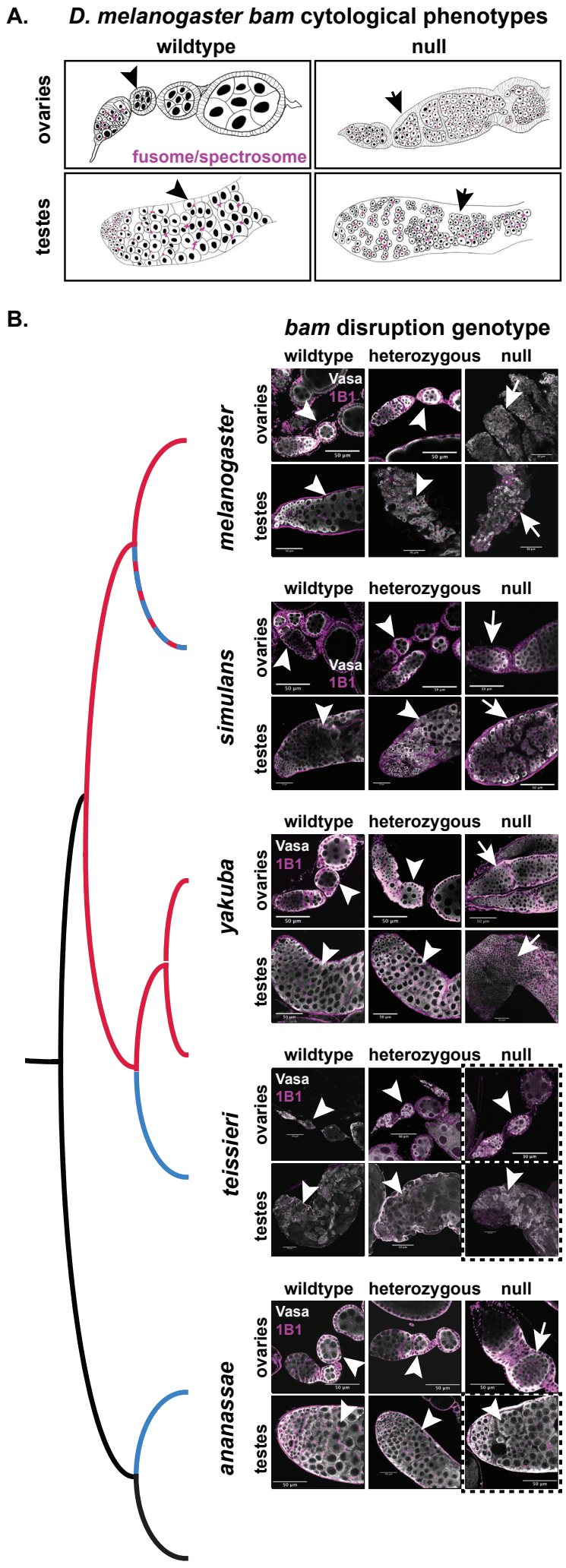
A.
D. melanogaster bam cytological phenotypes
wildtype
null
ovaries
testes
fusome/spectrosome
B.
bam disruption genotype
wildtype
heterozygous
null
melanogaster
simulans
yakuba
teissieri
ananassae
ovaries
testes
Vasa
1B1

Fig4

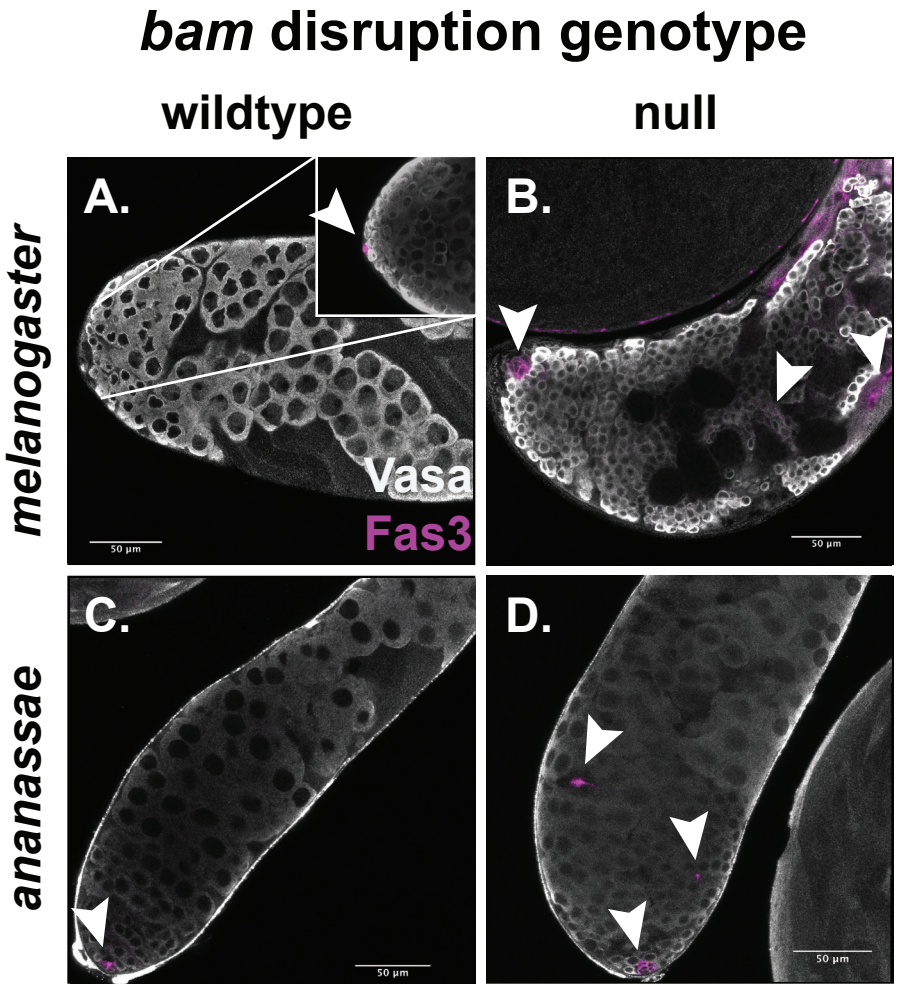
bam disruption genotype
wildtype
null
melanogaster
ananassae
A.
B.
C.
D.
Vasa
Fas3
50 µm
50 µm
50 µm
50 µm

Fig5

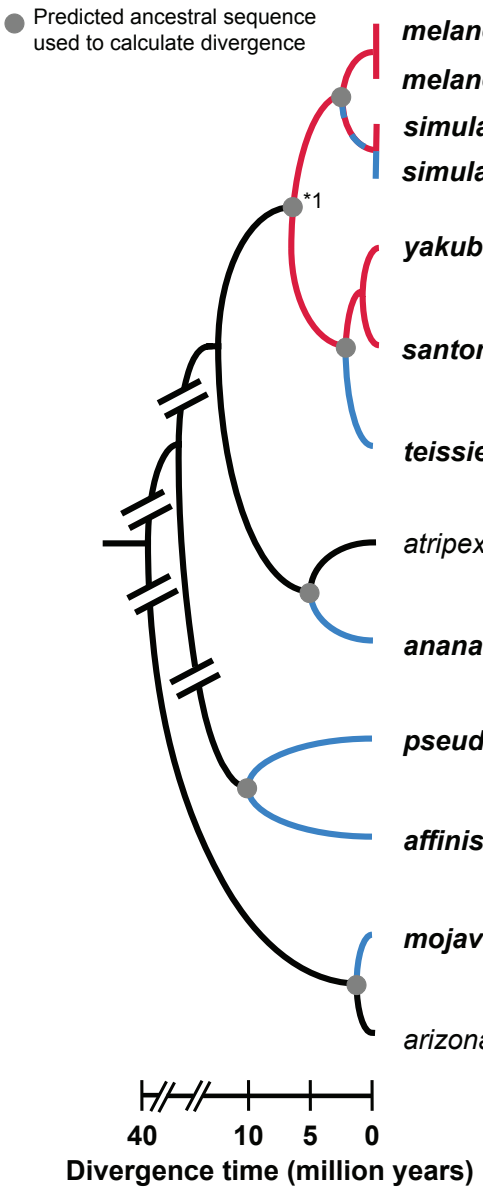

	Divergence		Polymorphism				
	N	S	N	S	alpha	P-value	n
***melanogaster* - ZM**	20	6	4	13	0.907	***0.000***	187
***melanogaster** - US, ZI*[1]	28	11	8	14	0.776	***0.008***	12,7
***simulans** - US, NC*[1]	26	16	9	15	0.631	***0.049***	10
***simulans* - US, CA**	46	25	13	15	0.528	0.093	182
***yakuba*- Bioko**	26	18	10	25	0.723	***0.006***	14
***santomea*- São Tomé**	24	21	5	16	0.726	***0.024***	11
***teissieri*- Bioko**	12	13	14	15	-0.011	0.983	11
atripex							
***ananassae* - Thailand**[2]	28	36	1	7	0.816	0.089	14
***pseudoobscura* - US, CA**	40	41	3	6	0.487	0.360	11
***affinis* - US**	31	31	5	7	0.285	0.597	14
***mojavensis* - US**	2	5	3	8	0.250	1	22
arizonae							

Fig S1

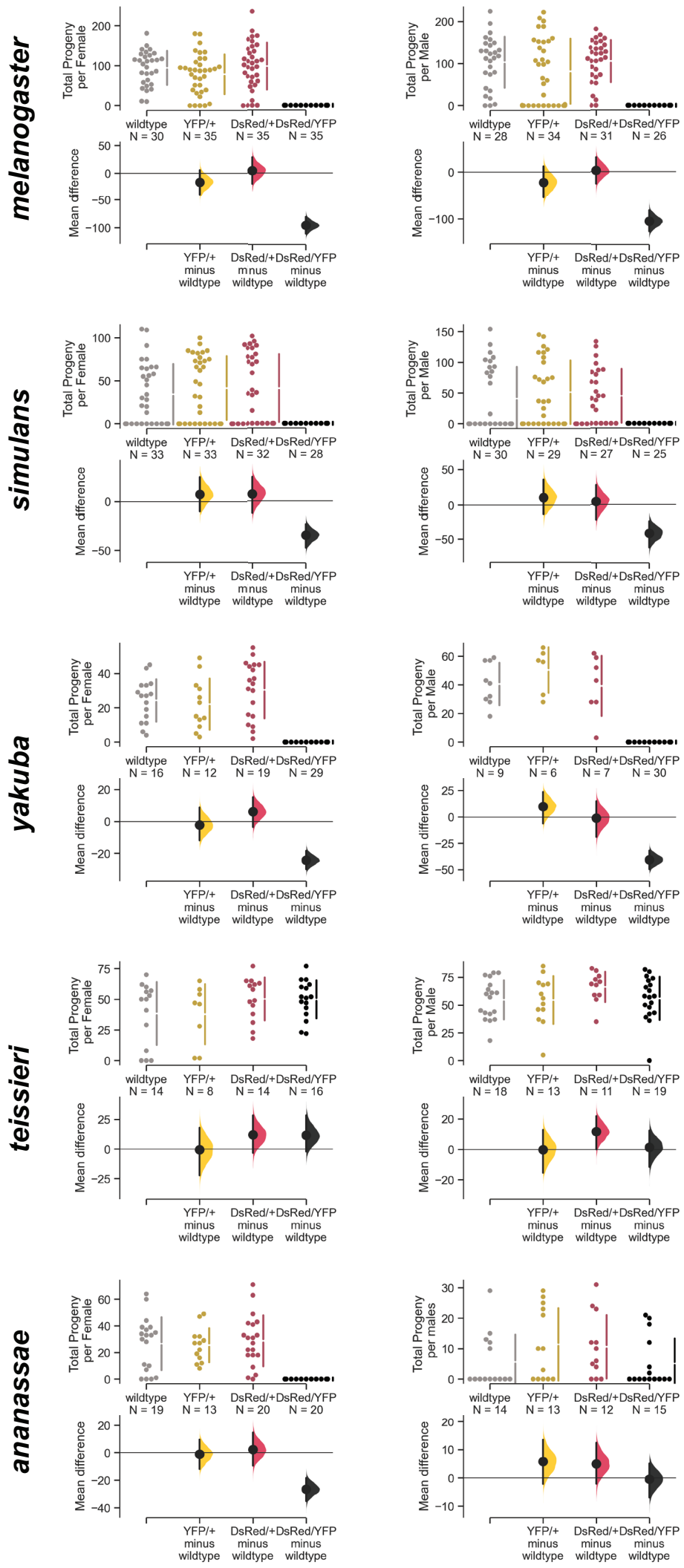
melanogaster
Total Progeny per Female
wildtype N = 30
YFP/+ N = 35
DsRed/+ N = 35
DsRed/YFP N = 35
Mean difference
YFP/+ minus wildtype
DsRed/+ minus wildtype
DsRed/YFP minus wildtype
Total Progeny per Male
wildtype N = 28
YFP/+ N = 34
DsRed/+ N = 31
DsRed/YFP N = 26
simulans
wildtype N = 33
YFP/+ N = 33
DsRed/+ N = 32
DsRed/YFP N = 28
wildtype N = 30
YFP/+ N = 29
DsRed/+ N = 27
DsRed/YFP N = 25
yakuba
wildtype N = 16
YFP/+ N = 12
DsRed/+ N = 19
DsRed/YFP N = 29
wildtype N = 9
YFP/+ N = 6
DsRed/+ N = 7
DsRed/YFP N = 30
teissieri
wildtype N = 14
YFP/+ N = 8
DsRed/+ N = 14
DsRed/YFP N = 16
wildtype N = 18
YFP/+ N = 13
DsRed/+ N = 11
DsRed/YFP N = 19
ananassae
wildtype N = 19
YFP/+ N = 13
DsRed/+ N = 20
DsRed/YFP N = 20
Total Progeny per males
wildtype N = 14
YFP/+ N = 13
DsRed/+ N = 12
DsRed/YFP N = 15

Fig S2

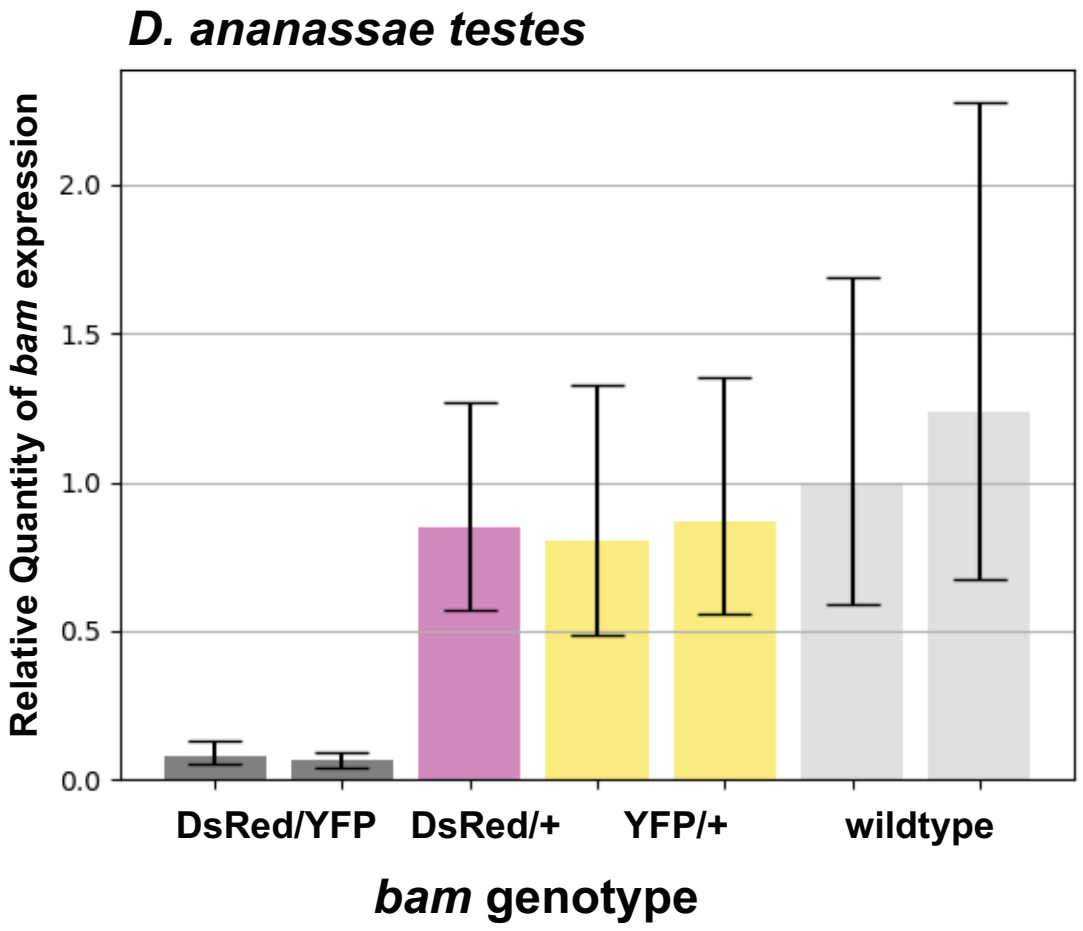
D. ananassae testes
Relative Quantity of bam expression
2.0
1.5
1.0
0.5
0.0
DsRed/YFP
DsRed/+
YFP/+
wildtype
bam genotype

Fig S3

A. *D. teissieri* ovaries

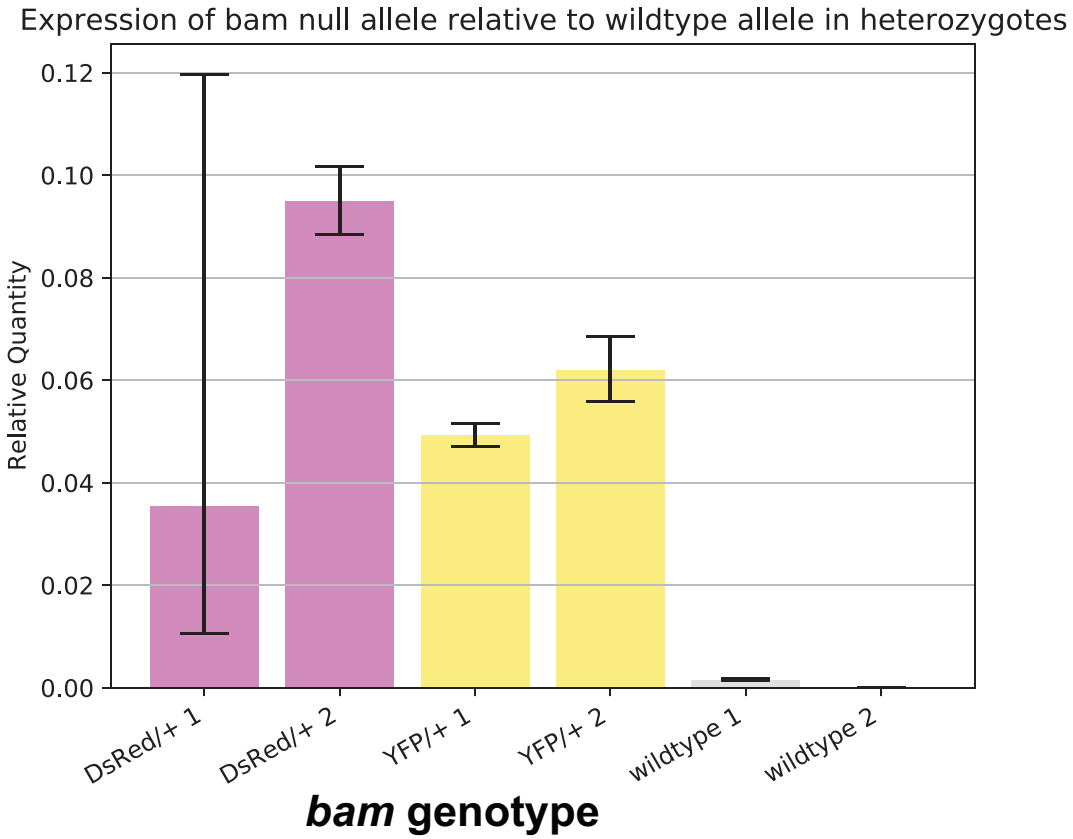

B. *D. teissieri* testes

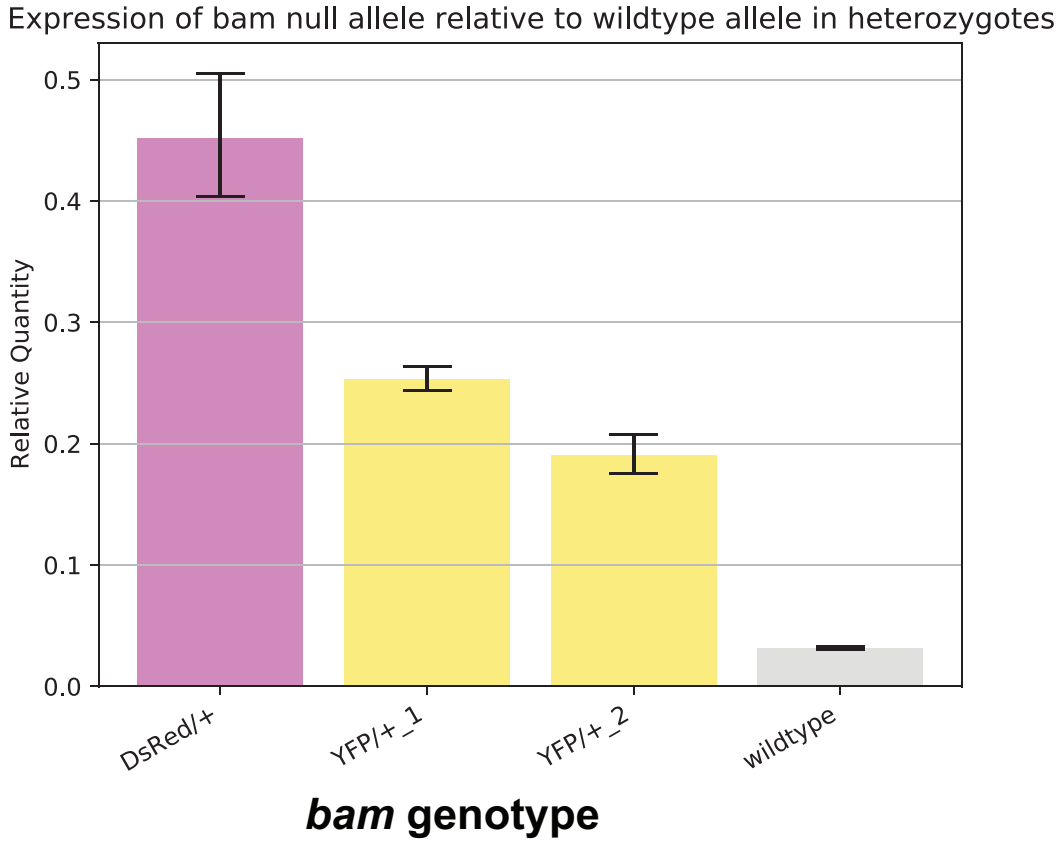

Fig S4

A. *D. teissieri* ovaries

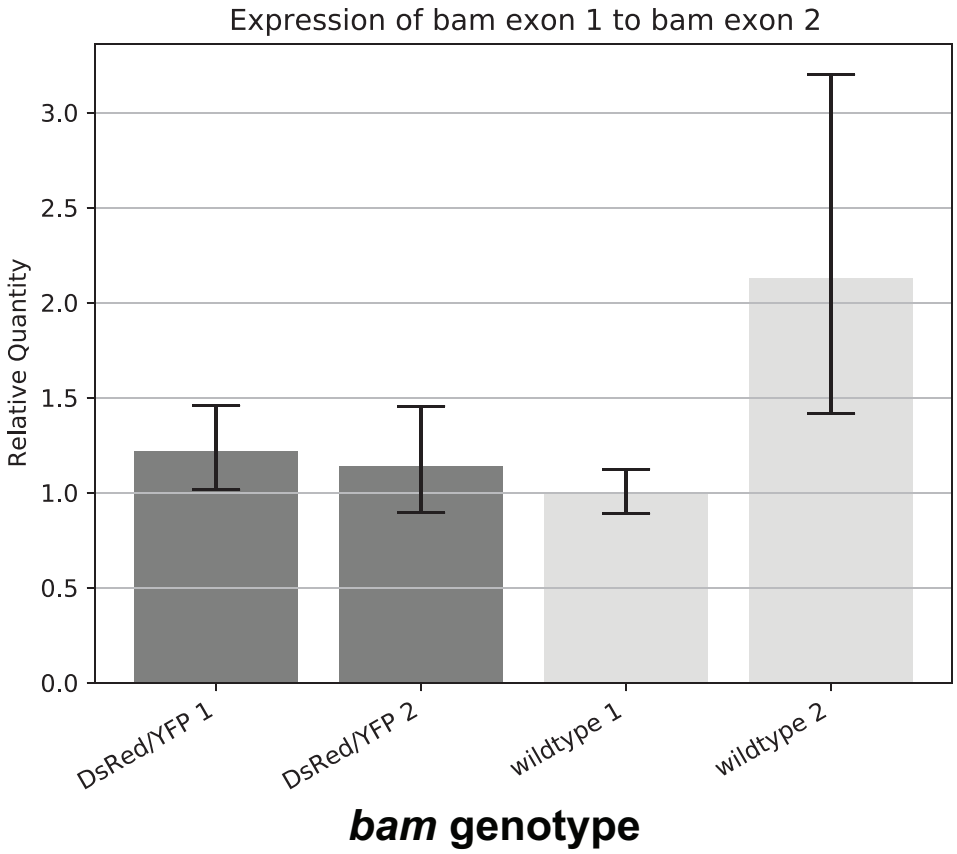
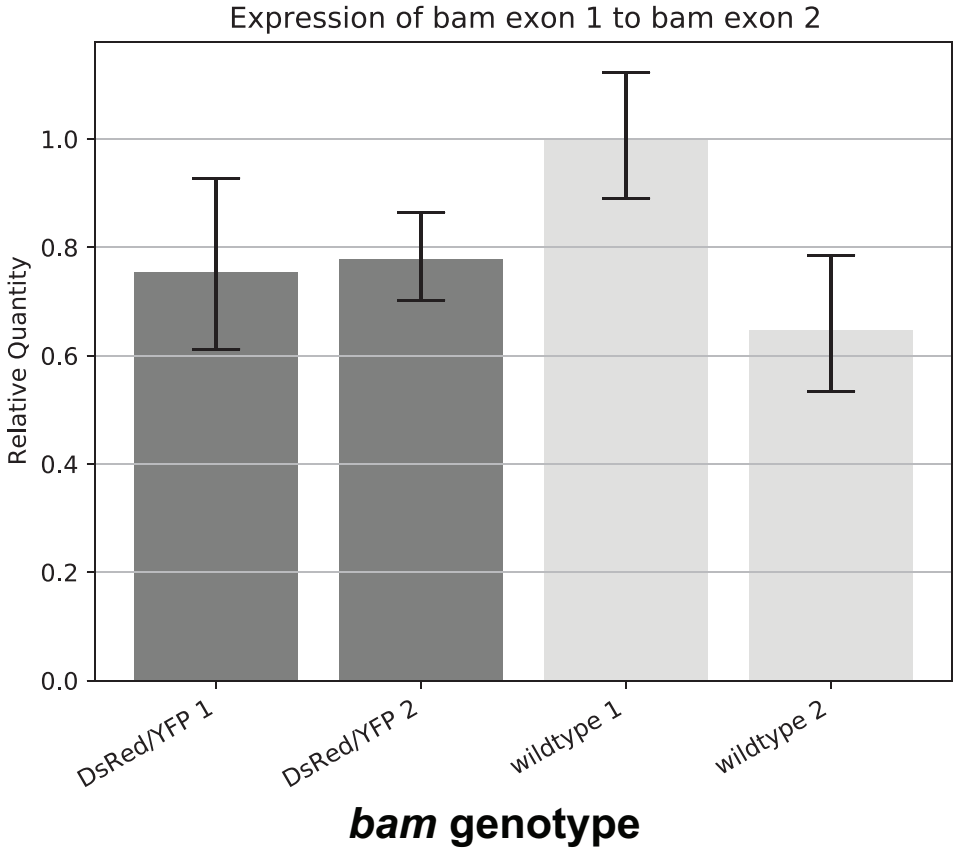
B. *D. teissieri* testes